REVIEW PAPERS

Polymer matrix nanocomposites for heavy metal adsorption: a review

Gholamhossein Mohammadnezhad[1] · Arnavaz Keikavousi Behbahan[2]

Abstract
Heavy metals belong to a group of lethal environmental pollutants. Ongoing efforts targeted at safeguarding public health have led to considerable attention being focused on methods that allow efficient extraction of these toxic substances. Polymer nanocomposites (PNCs) with their special characteristics are a class of adsorbents that demonstrate high potential for use in heavy metal extraction. As this process of removal is predominantly governed by adsorption, various parameters in PNCs' chemical structure, as well as the metal solutions, can have a significant effect on the adsorption process. Herein, this review undertakes a survey of recently developed PNCs and their metal adsorption studies.

Keywords Nanocomposite · Inorganic nanofiller · Polymer matrix · Heavy metal removal · Adsorption · Water treatment · Surface modification

Abbreviations

AA	Acrylic acid
AgNPs	Silver nanoparticles
ALG	Alginate
AM	Acrylamide
APS	Ammonium peroxodisulfate
APTS	3-Aminopropyltriethoxysilane
ATP	Attapulgite
ATP/FA/Poly(AA-co-AM)	Attapulgite/fly ash/poly(acrylic acid-co-acrylamide)
ATP/Poly(AA-co-AM)	Attapulgite/poly(acrylic acid-co-acrylamide)
BSA	Bovine serum albumin
BT	Bentonite
CA	Chlor-Alkali
CC	Calcium carbonate
CDVS	Chlorodimethylvinylsilane
CMWCNT	Carboxylated multi-walled carbon nanotube
CM-β-CD	Carboxymethyl-β-cyclodextrin
CNTs	Carbon nanotubes
Co	Cobalt
Cs	Caesium
CS	Chitosan
CSMV	Chitosan/starch–MWCNT–LVA
CTS–PVA/BT	Chitosan–poly(vinyl alcohol)/bentonite
DA	Diacid
DHAQ	1,8-Dihydroxyanthraquinone
DHB	3,4-Dihydroxybenzene
EDTA	Ethylenediaminetetraacetic acid
EtOH	Ethanol
Eu	Europium
FA	Ferulic acid
GA	Glutaraldehyde
GG-g-PAM	Guar gum grafted with poly(acrylamide)
HMS	Hexagonal mesoporous silica nanoparticle
HNC	Hydrogel nanocomposites
HSAB	Hard and soft acid and bases
I-LDH	Intercalated LDH
LDH	Layered double hydroxide
LVA	L-valine
mB	Modified boehmite

✉ Gholamhossein Mohammadnezhad
mohammadnezhad@iut.ac.ir; g_m1358@yahoo.com

1   Department of Chemistry, Isfahan University of Technology, Isfahan 84156-83111, Islamic Republic of Iran

2   Environmental and Bio–Analytical Laboratories, Department of Chemistry, Sharif University of Technology, P.O. Box 11365–9516, Tehran, Iran

MBA	N-Methylenebisacrylamide
MBNC	Modified nano-boehmite and poly(methyl methacrylate)
MNC	Magnetic nanocomposite
MNP	Magnetic nanoparticle
MPTS	3-Mercaptopropyl trimethoxysilane
MWCNT	Multi-walled CNTs
N	Nitrogen
NC	Nanocellulose
NRs	Nanorods
NY6	Nylon-6
pH_{ZPC}	Zero point charge pH
PAAm	Poly(acrylamide)
PAM	Polyacrylamide
PAN	Polyacrylonitrile
PANI	Polyaniline
PANI-SnSiP	Polyaniline-Sn(IV) silicophosphate
PG	Percentage of grafting
PMMA	Poly(methyl methacrylate)
PMNCs	Polymer matrix nanocomposites
PNCs	Polymer nanocomposites
PPy	Polypyrrole
PPy/SH-Beta/MCM-41	Polypyrrole/thiol-functionalized Beta/MCM-41
PS	Polystyrene
PVA	Poly(vinyl alcohol)
PVC	Polyvinylchloride
PVP	Poly(vinyl pyrrolidone)
QD	Quantum dot
rec-PET	Recycled polyethyleneterephthalate
SA	Stearic acid
Si	Silica
SNHS	Silica nano hollow sphere
SSS	Styrene sodium sulfonate
TEOS	Tetraethyl orthosilicate
TG	Tragacanth gum
TGA	Thermogravimetric analysis
US EPA	United States Environmental Protection Agency
WHO	World Health Organization

Introduction

Nowadays, human health is under threat from various harmful organic and inorganic compounds. Among these, metals are a group of pollutants that present a greater risk because even at trace levels they still demonstrate a potent peril from their presence [1–4]. Therefore, finding effective systems to remove undesirable metals remains a challenging task for scientists. Continuing research efforts have resulted in the development of diverse methods for heavy metal removal including chemical precipitation, ion exchange, adsorption, electrochemical technologies, etc. [5–7]. Among these methods, adsorption has shown high efficiency and flexibility in its application mostly due to the several controllable parameters such as diverse chemical structure, surface modification, and film forming. For maximal utilization, high adsorption as well as simple, effective desorption conditions are generally preferred and should be optimized, and all under mild conditions. In the case of desorption, this is to enable repeated use of the adsorbents, thereby reducing economic costs.

Among the vast varieties of existing adsorbents, polymer-based nanocomposites have recently been the subject of interest from researchers stemming from the high potential they show. This new class of hybrid materials called PNCs is typically obtained via a combination of organic polymer and inorganic nanofillers. Unique properties of polymers such as flexibility, ductility, and processability in addition to the advantages of inorganic nanofillers such as rigidity, and thermal stability [8] are combined in the PNCs. Interestingly, nanofillers can alter the macroscopic properties of polymers even at very low concentrations [9]. One such property over which they exert a strong influence is the large surface area typically associated with PNCs, thereby making them a great candidate for adsorption studies [8, 10, 11].

This review summarizes the recent studies on metal ion removal by focusing on PNCs as adsorbents based on the published papers.

Application of PNCs in the removal of metals
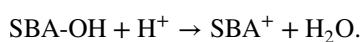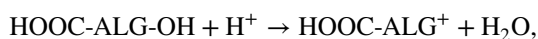
Lead ions adsorption

Being a ubiquitous toxic metal, lead largely presents a widespread environmental issue due to its tendency of accumulating in bone, liver, brain, kidney, and muscle. Since it can cause severe problems such as mental retardation, anemia, and kidney diseases, the World Health Organization (WHO) has proposed limiting the concentration level of lead in water to 10 $\mu g\,L^{-1}$ [12]. Thus, efforts have been made to find a way to adequately remove lead from water.

Lead is typically found in its Pb^{2+} and Pb^{4+} forms in solution media. As a result of its possession of positive charges in aqueous media, the extractant phase must have functional groups on its surface that contain negative charges as the pH increases, in order to attract the lead ions.
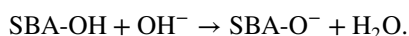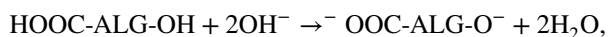
The discovery of the triblock copolymer-templated SBA-15 has opened up avenues to perform fascinating experiments within the resulting channel structures.

SBA-15 with its large, tunable pore sizes, and highly ordered hexagonal topology has also been frequent subject material of interest in these groups of studies [13, 14]. In an investigation carried out by Cheraghali et al., SBA-15 with alginate (ALG) [$(C_6H_8O_5)_n$] was utilized as a new PNC adsorbent. Since alginate possesses carboxylic and hydroxyl groups within its structure, sufficient negative charge can be generated via pH adjustment of the solution. It has been generally observed that during pH modification, a sudden increase in the adsorption of lead ions between pH 2 and 3 takes place. Subsequently, the authors proposed specific reactions occurring at the different pH values, which are summarized as follows:

Acidic medium:

$$HOOC\text{-}ALG\text{-}OH + H^+ \rightarrow HOOC\text{-}ALG^+ + H_2O,$$

$$SBA\text{-}OH + H^+ \rightarrow SBA^+ + H_2O.$$

Basic medium:

$$HOOC\text{-}ALG\text{-}OH + 2OH^- \rightarrow^- OOC\text{-}ALG\text{-}O^- + 2H_2O,$$

$$SBA\text{-}OH + OH^- \rightarrow SBA\text{-}O^- + H_2O.$$

From the above, a satisfactory conclusion is that pH adjustment plays an important role in the adsorption of metal ions and of lead in particular. Increasing the pH leads to the functional groups occurring mainly in their negative forms. In addition, this reduces the competition between the Pb^{2+} and H^+ ions on adsorption sites, resulting in an increase in lead adsorption. It must, however, be noted that lead can precipitate or form complexes in solutions at high pH values, which interferes with the extraction process. In this specific study, the optimized pH value was estimated and reported to be 5.6 [15].

One way to enhance adsorption is by altering functional groups in the structure of the sorbents. In this way, Wang et al. used SiO_2–NH_2 and PAM (polyacrylamide) to prepare the sorbent via radical polymerization. The adsorption ability of the resulting adsorbent toward Cu(II), Cd(II), and Pb(II) ions was then studied. The most important point in this study is the prominent role, which the SiO_2–NH_2 functional group plays and it was found that increasing the number of SiO_2–NH_2 units in the PNCs not only helped the polymerization, but also enhanced the adsorption ability. It is thus safe to conclude that SiO_2–NH_2 performs a more important function in the adsorption capacity compared to pure PAM. As previously mentioned, pH adjustment plays a crucial role in the adsorption of metal ions. Therefore, in this particular instance, pH increase allows the metal ions to form chelates with the –NH_2 units present in the SiO_2–NH_2

functional groups [16]. On a supplementary note, experimental evidence supports increased adsorption capacity of lead compared to the theoretical data. This would suggest observation of a synergistic influence of PAM, aside from the fact that it does not have proper functional groups to adsorb metal cations [17, 18]. As noted earlier, reusability of a sorbent offers great economic advantages and this greatly depends on the extent of desorption of the extractant, thereby avoiding the memory effect. In the aforementioned article, metal desorption was performed using HCl solution. Wang et al. [16] were able to desorb the metal up to 97 percent, implying that the sorbent can be assumed as economically suitable for utilization.

Jiang et al. [19] prepared a suitable sorbent with diverse functional groups. They activated attapulgite nanorods (ATP) and magnetic fly ash and then modified them using KH-570 (which is a coupling agent, γ-methacryloxyprop yltrimethoxysilane). Subsequently, the product was used as a cross-linker for the in situ inverse suspension copolymerization of acrylic acid (AA) and acrylamide (AM). SEM image of prepared ATP/FA/Poly(AA-co-AM) ternary nanocomposite and applying an external magnetic field on the PNC is shown in Fig. 1. This sorbent could then adsorb metal ions such as Pb, Zn, Cd, Cu and Ni through two different processes, chelate formation and ion exchange. Specifically, this sorbent showed a high adsorption capacity for lead ions, because of two reasons: first, the formation of stable chelates between Pb ions and nitrogen-containing functional groups and second, the electrostatic attraction between Pb and carboxylic functional groups [20]. In addition, the balanced presence of carboxyl and amido groups in the prepared adsorbent has enhanced water adsorption, thus enabling better metal extraction. Increasing the pH also boosted the extraction of lead cation due to the charge alteration of functional groups present on the walls of the adsorbent [21–23]. It was also observed to lead to decreasing the chloride concentration while extra non-chelated lead cations could be found in the extraction solution [24]. Finally, a pH around 6 was estimated as the optimal value. In this article, the effect of extraction time was also studied and two growing trends became apparent. The first trend is seen from the adsorption of Pb on the surface functional groups, while the second one is related to the permeation of Pb from the surface to the inner sorbent layers according to the osmotic effect. The process of desorption was also studied using an optimized concentration of HCl. Here, the hydronium ion replaces Pb^{2+} and saturates carboxylic functional group [25], while Cl^- reacts with Pb^{2+} and aids the desorption process. Reusability tests also showed decreases of less than 2 mg g^{-1} and 2% during five cycles of adsorption and desorption, respectively, which would suggest that the ATP/FA/Poly(AA-co-AM) microgel is reusable.

Fig. 1 SEM image of ATP/FA/Poly(AA-co-AM) ternary nanocomposite and beside application of external magnetic field on it [19]
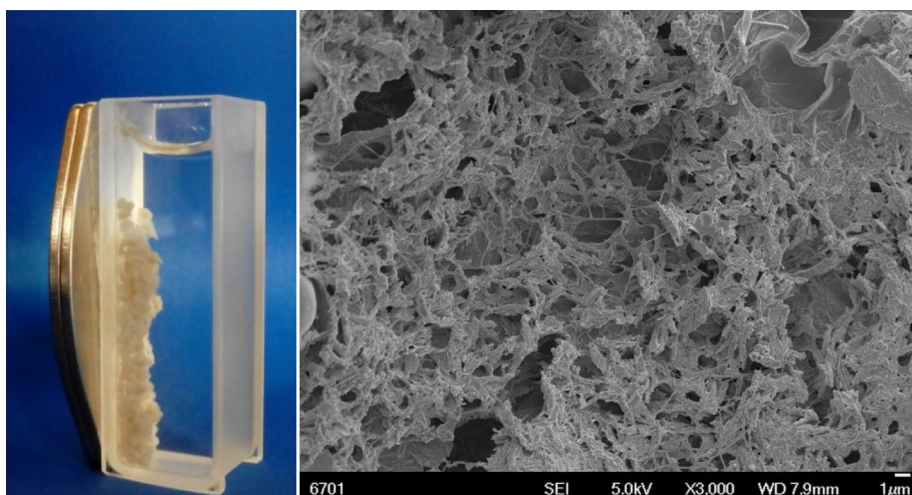
In 2014, Liu et al. were able to synthesize an adsorbent, which showed structural similarities to that already reported by Jiang et al. [19]. In their study, they also utilized ATP as the substrate and the activation process was performed by immersion in 0.1 M HCl for 24 h. Afterward, the activated substrate was kept in liquid paraffin combined with Span-80 and Tween-60. They also used KH-570 as a surfactant. The modified ATP (ATP–C=C) was utilized in the suspension polymerization of AA and AM to make the final sorbent, ATP/Poly(AA-co-AM). The effect of (A) ATP–C=C/AA–AM, (B) Span-80/Tween-60, (C) % APS (ammonium persulfate), and (D) oil–water ratio was studied in an

orthogonal experimental design (Table 1), with a total of nine samples being prepared [26]. The adsorption potential of all prepared nine ATP/Poly(AA-co-AM) PNCs was then studied using Cu as model metal. Low copolymer percentage and high amount of initiator/cross-linking agent in samples 8 and 5, respectively, resulted in a low percentage of grafting (%PG), and accordingly, they exhibited the lowest metal uptake [27]. Also, it was possible to infer from the extraction potential of the prepared PNCs that surfactant use was the most effective while oil-to-water ratio was the least effective parameter on the adsorption of Cu^{2+}. Finally, sample 1 was chosen as the optimized PNC sorbent and its selectivity

Table 1 $L_9(3^4)$ Orthogonal experiment design for the ATP/P(AA-co-AM) nanocomposite hydrogels [26]

Level	Variables			
	A ATP–C=C/(AA + AM)	B[a] Span-80/Tween-60	C APS% (%)	D oil–water ratio
Arrangements for orthogonal test of four-variable three-level variables				
1	1:5	1:0	0.5	2:1
2	1:7	1:1	1.0	3:1
3	1:9	0:1	1.5	4:1
Serial number	Variables			
	A	B	C	D
Array of the four-variable three-level orthogonal experiments				
1	1	1	1	1
2	1	2	2	2
3	1	3	3	3
4	2	1	2	3
5	2	2	3	1
6	2	3	1	2
7	3	1	3	2
8	3	2	1	3
9	3	3	2	1

[a]The total amount of Span-80 and Tween-60 is 5% of water

was studied using five metals including Ni, Cu, Cd, Zn, and Pb. The obtained results illustrate a clear selectivity of this sorbent for Pb^{2+} [28] and Cu^{2+} [29]. The presence of AM within the structure of sorbent facilitated its chelation with Cu^{2+} through amide groups.

As usual, the effect of pH was investigated and increment of metal adsorption was observed to accompany pH increase. At values higher than 6, lead forms $PbCl_4^{2-}$ and $PbCl_3^-$ and precipitates as $PbCl_2$ which is unfavorable. Thus, optimized pH for Cu and Pb metal ions was reported 4 and

Fig. 2 Heavy metal removal mechanism by PANI-SnSiP [30]

6, respectively. Desorption time and acid concentration were also optimized. A 100% desorption can be expected by a 0.2 M HCl and 2 h of desorption time. Therefore, sample 1 can be used several times according to its sufficient adsorption and desorption ability. But unfortunately, the cyclability of this sorbent was not considered [26].

In 2014, Anees Ahmad and his co-workers prepared an adsorbent using Sn(IV) silicophosphate inorganic precipitate (made from orthophosphoric acid, sodium silicate, and stannic chloride) utilizing PANI (polyaniline) as the substrate (PANI-SnSiP). The suggested steric structure of this sorbent is illustrated in Fig. 2. Interestingly, the sorbent showed selective extraction of Pb, Hg, and Co ions due to the adequate functional groups present in its structure, but surprisingly no optimization was performed by the authors. As an optional factor, it was reported that PANI-SnSiP has shown good performance in dye adsorption and antibacterial activity [30].

Simultaneous adsorption of Pb, Ni, and Cd ions was studied in an interesting article in 2013 [31]. In this study, Badruddoza et al. synthesized a carboxymethyl-β-cyclodextrin (CM-β-CD) polymer modified with Fe_3O_4 nanoparticles (CDpoly-MNPs) (Fig. 3). Afterward, they investigated the effect of pH on adsorption of Pb, Cd, and Ni ions and stated that the enhancement of metal ion adsorption by pH is related to zero point charge pH (pH_{ZPC}). The pH_{ZPC} for this sorbent is 4.4, and at values greater than this point, carboxylic groups typically adopt a negative form and have a strong electrostatic attraction toward positive metal ions. At lower pH values, carboxylic groups are present in their protonated forms and this can lead to competition between metal ions and H^+, thereby diminishing their metal uptake capacities. In spite of enhanced metal adsorption accompanying pH increment, hydroxylation of metal ions occurs in pH greater than 6. Therefore, the optimized pH was reported to be 5.5 [32].
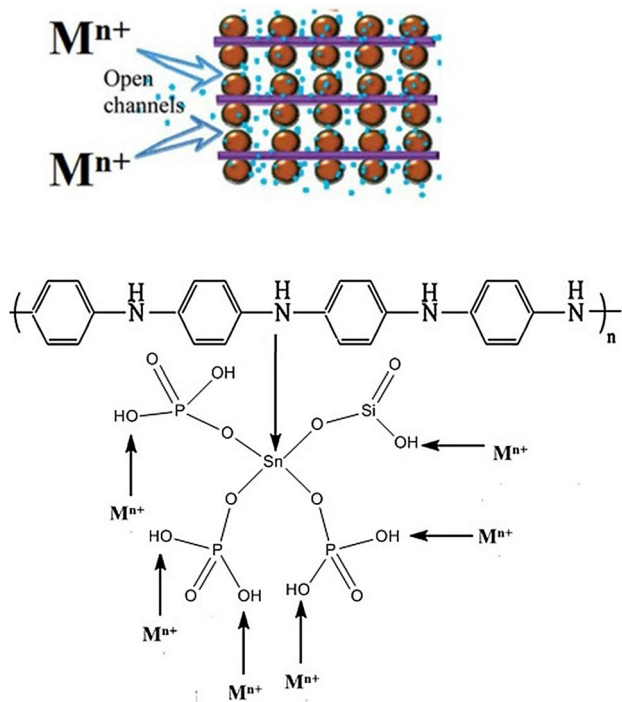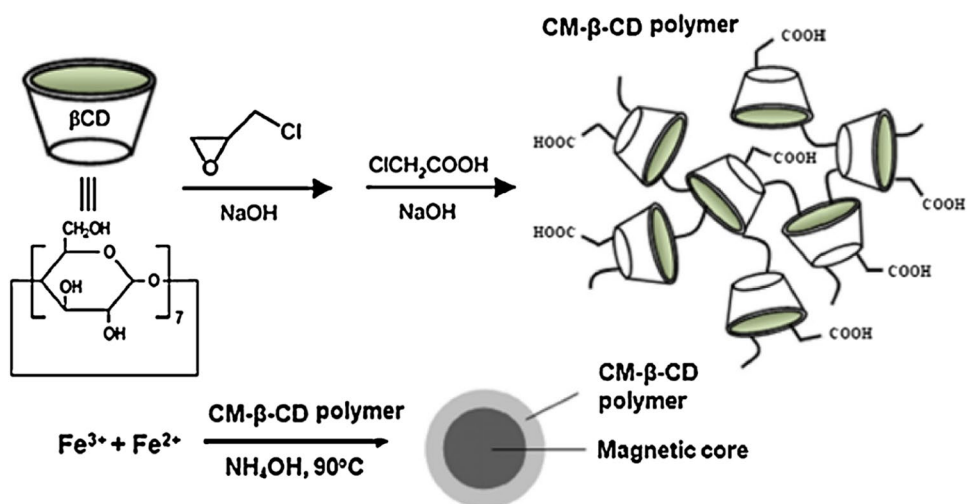
Fig. 3 Schematic presentation of CM-β-CD polymer grafting on Fe_3O_4 nanoparticles [31]

Lim et al. prepared a nanocomposite using polypyrrole (PPy) and silica in 2012 in order to investigate the adsorption of several metal ions including Pb^{2+}, Cd^{2+}, Cu^{2+}, Ni^{2+}, Cr^{3+}, Ag^{+}, and Hg^{2+}. The authors reportedly used colloidal silica (Ludox SM-30, average particle size 7 nm) as a template in preparing the PPy/silica nanocomposite while its surface was modified using chlorodimethylvinylsilane (CDVS). The polypyrrole polymerization was initiated using $FeCl_3$. Finally, the silica particles were eliminated using NaOH solution revealing a cratered surface (Fig. 4) [33]. As seen from the TEM images of the polypyrrole (PPy)/silica nanocomposites (Fig. 4), the structure contains well-arranged holes, which presents proof of its accessible surface and eventually its adsorption capability. They also observed that the nanocomposite's tendency to adsorb Hg^{2+}, Ag^{+}, and Pb^{2+} was greater than Cu^{2+}, Ni^{2+}, Cd^{2+}, and Cr^{3+}, an observation which was explained using hard and soft acid and bases (HSAB) theory. Since Hg^{2+}, Ag^{+}, and Pb^{2+} are considered as soft Lewis acids, they easily form stable complexes with soft bases like secondary amines present in polypyrrole structure. In adsorption competition between

these three soft Lewis acids, an order of $Ag^{+} > Hg^{2+} > Pb^{2+}$ was observed [34, 35]. Desorption with HCl solution was also studied, and a capacity of 95% was observed that could be beneficial for the nanocomposite's usage in practical wastewater recycling. Since no optimization of adsorption and desorption conditions through pH adjustment was performed in this article, the optimal extraction potential of this sorbent is still unknown.

Nanocellulose (NC) is a new class of cellulose material, which has excellent physicochemical properties and an eco-friendly nature with wide application prospects that have attracted much attention in recent years. In 2012, Suman et al. prepared a novel reusable cost-effective water purification device for complete removal of dyes, heavy metals, and microbes, using NC and silver nanoparticles (AgNPs)-embedded pebbles-based composite. They filled a column and used it for separation and simultaneous removal of dye (methylene blue), heavy metals (lead and trivalent chromium) and microbes (Escherichia coli). They observed that the column could adsorb heavy metals sufficiently for 6 tandem extractions and desorption processes without any significant decrease in adsorption efficiency [36]. It has been revealed that the NC part of the column is responsible for heavy metal adsorption due to its carboxylic and hydroxyl functional groups [37–40]. Also, the pH was justified and an increase in heavy metal adsorption from 2 to 4 was observed, which correlates with the appearance of anionic functional groups as the pH increases. Through their studies, they were able to determine the optimum pH to be around 6, which is the highest possible pH without heavy metal precipitation [41, 42].

High surface area, availability, and cheapness have made the nanostructural MnO_2 an auspicious nominee for energy storage, catalysis, NCs fabrication, and so on [43]. Mallakpour et al. were able to perform comprehensive studies on PNCs using MnO_2 as filler during 2016–2018 and investigated their metal adsorption capability with lead as the target analyte. Different linkages of the octahedral MnO_6 units can lead to α, β, γ, and δ MnO_2 types. Among them is the α-type, which is assembled from double chains octahedrals, thereby forming 2×2 tunnels and making it practical for intercalation processes [44–46]. Modifying polymers with neat α-MnO_2 can, therefore, enhance PNCs characteristics although interparticle connections, i.e., hydrogen bonding between nanoparticles, can lead to their agglomeration, a fact which could undermine the resulting films' properties by disrupting the homogenous dispersion of fillers. Thus, it is necessary to modify the nanofiller prior to their utilization. In 2016, Mallakpour et al primarily synthesized MnO_2 by the solvothermal method and then functionalized α-MnO_2 nanorods with γ-aminopropyltriethoxysilane (KH550). Chitosan (CS) as a biodegradable, cheap, and the non-toxic polymer was used for preparing the PNC by the
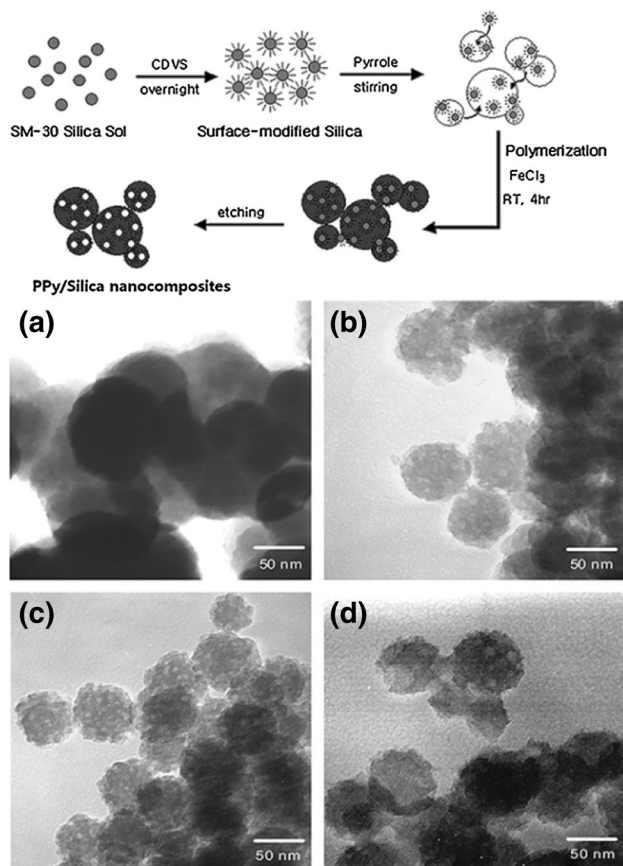

Fig. 4 An illustration of PPy/silica nanocomposites preparation and TEM images of PPy/silica nanocomposites synthesized with **a** 0, **b** 2, **c** 4, and **d** 6 mL SM-30 silica sol solution [33]

ultrasonic-assisted technique with the expectation that the amine groups present on CS surface can aid metal adsorption properties of the resulting composites. Due to the solubility of CS under acidic conditions (pH < 3), varying quantities of glutaraldehyde (GA) (0, 0.125, 0.25, 0.5, and 1%) were used as cross-linkers not only to stabilize CS in acidic conditions but also to enhance its mechanical properties. Nevertheless, utilization of GA can result in the amine groups being cross-linked, thus reducing the associated PNC's metal extraction capacity. Even though adsorption studies were performed at neutral pH, they were able to prove that using KH550-modified-α-MnO$_2$ as a filler beside GA-cross-linked CS ignores the detrimental effect of amine group deactivation and results in increasing Pb(II) adsorption [47]. In another study [48], they used KH550-modified MnO$_2$ (1, 3, and 5 wt%) along with polyvinylchloride (PVC), which enhanced the latter's thermal and mechanical properties while improving the PNC's lead adsorption capability. Expectedly, the prepared adsorbent showed an extraction capacity of 100 mg g^{-1}, which is quite reasonable. Poly(vinyl alcohol) (PVA), as a non-carcinogenic, biodegradable, and remarkable water-soluble polymer, has also found usage beside MnO$_2$–KH550-modified nanofiller (1, 3, and 5 wt%) by Mallakpour et al. The resulting NC had an adsorption extraction of 32.4 mg g^{-1}, which was reported to be higher than that obtained from neat PVA (26.4 mg g^{-1}) [49].

They also modified α-MnO$_2$ by L-valine (LVA) and used it alongside PVA for preparing the desired nanocomposite. LVA is an eco-friendly amino acid with the carboxylic acid functional group, which then reacts with the OH-rich external surface of the α-MnO$_2$ nanorods (NRs), thereby improving dispersion. PVA/α-MnO$_2$–LVA metal adsorption behavior was investigated using Pb(II) and Cd(II) in their respective salt solutions at neutral pH. According to their report, the present amine (LVA) and hydroxyl (Mn–OH) functional groups act as chelating agents and enable good metal extraction by a metal chelation mechanism [50]. They also used LVA-modified-α-MnO$_2$ (1, 2, and 3 wt%) with CS and investigated its lead extraction capability [51]. As the CS was unmodified in this instance, adsorption studies were performed in neutral pH. They found that LVA–α-MnO$_2$/CS displayed greater metal adsorption ability (163.93 mg g^{-1}) compared to other proposed PNCs including those they already reported in previous studies (16.45 mg g^{-1}) [50]. In addition, varying the amount of LVA-modified α-MnO$_2$ processed with PVC and PNC led to an optimal content of 5 wt% being determined, wherein the best thermal and mechanical properties were observed, which was then used for further metal adsorption studies. For their metal extraction studies, the effect of pH (value range 3–7), quantity of adsorbent (20–100 mg) and primary Pb(II) concentration (20–100 mg L^{-1}) was considered and a final extraction

ability of 50 mg g^{-1} was estimated under optimum conditions [52]. Eventually, these results indicate that synchronized usage of the aforementioned polymers in conjunction with modified α-MnO$_2$ can increase lead adsorption while compensating for the polymers' mechanical and thermal defects.

Carbon nanotubes (CNTs) possess a high aspect ratio as well as strong *van der* Waals forces. However, this can cause strong attractions between the nanotubes, which could result in them being poorly compatible with polymers. To this end, Mallakpour et al. modified the surface of multi-walled CNTs (MWCNT) using bovine serum albumin (BSA), which is one of the most widely studied proteins and is present in the body fluids of vertebrates. Recycled polyethylene terephthalate (rec-PET) was then used as the substrate, and characterization of the prepared 2 wt% PNC showed a good dispersion of nanofiller within the polymer matrix. Metal adsorption investigations on rec-PET/MWCNT–BSA 2 wt% revealed a maximum extraction capacity of 22.47 mg g^{-1} [53].

Recently, Malakpour et al. also reported ultrasound-assisted preparation of a new PNC–hydrogel nanocomposite (HNC), containing calcium carbonate nanoparticles (CC) as filler and tragacanth gum (TG) as substrate. Just as expected, improved thermal stability, H-bonding breakage, and subsequent dissociation of aggregated NPs were observed. According to the BET results, TG/CC HNC 5 wt% was classified as a mesoporous material arising from the pore size estimated at 7.85 nm. Additionally, the prepared nanocomposite showed the best performance for removal of lead ions at pH = 5 with an extraction time of 180 min and Pb(II) concentration level of 70 ppm using 0.015 g of biosorbent, which gave a removal efficiency of 192 mg g^{-1} [54].

Mercury ion adsorption

Mercury is one of the most potentially hazardous trace heavy metals commonly found in the global environment [55]. The natural outgassing of mercury from the earth's crust through volcanoes is the primary source of its introduction into the surface environment. Interestingly, mercury's toxicity strongly depends on its oxidation state, and the common, most toxic, and highly reactive form of this heavy metal is Hg(II). Since mercury causes injurious disorders, especially in the transmission of nerve impulses, US EPA (the United States Environmental Protection Agency) has included it in the list of priority pollutants with an obligatory limitation of 10 mg L^{-1} for wastewater [56]. Therefore, proposing an efficient sorbent to selectively adsorb mercury from water and wastewater is extremely crucial and necessary.

Production of nanofibers using electrospinning is currently a novel technique in preparing an adsorbent with the high surface area. In 2011, a selective sorbent was prepared using this method by Teng et al., and in their report, a

mesoporous polyvinylpyrrolidone composite, (PVP)/SiO$_2$, was functionalized with thioether groups and the nanofibers were supplied by electrospinning. They then used a controlled and optimized amount of BTESTPS ((CH$_3$CH$_2$O)$_3$Si(CH$_2$)$_3$S–S–S(CH$_2$)$_3$Si–(OCH$_2$CH$_3$)$_3$), and TEOS (tetraethyl orthosilicate) to functionalize the polymer. Its ability for heavy metal adsorption was then examined by immersion in aqueous solutions containing certain amounts of Hg(NO$_3$)$_2$.0.5H$_2$O, Cu(NO$_3$)$_2$3H$_2$O, Cr(NO$_3$)$_3$, Pb(NO$_3$)$_2$, and Zn(NO$_3$)$_2$6H$_2$O. According to the reported data, the sorbent exhibited a specific tendency to adsorb Hg(II) [57]. This was attributed to the sulfur atoms present on the surface of the sorbents, which are soft donor atoms. As such they eagerly adsorbed mercury, which is the softest acceptor metal among the heavy metals tested in this work. They also observed that increasing the BTESTPS amount led to an increase in the extraction of Hg, which supports the selectivity in mercury extraction displayed by this sorbent.

In 2011, Li et al. reported a new adsorbent incorporating PAN (polyacrylonitrile) and MPTS (3-mercaptopropyl trimethoxysilane). In their work, they electrospun PAN solution that was then immersed in a solution containing ethanol, 37% HCl, and MPTS several times to form a thiol-functionalized silica layer. Afterward, the PAN nanofiber templates were dissolved to obtain zonal mercaptopropyl silica nanofibers. (The procedure is shown in Fig. 5.) The SEM image of the sorbent completely showed higher surface area upon PAN removal (Fig. 6d). Metal adsorption was then investigated using Hg^{2+}, which can be taken up on the surface of the material by electrostatic interactions or chelate formation (coordination of lone-pair electrons from the matrices to metal ions). While optimal adsorption time was established at 30 min, other parameters affecting adsorption were unfortunately not optimized in this research [58].

In 2013, a hexagonal mesoporous silica nanoparticle (HMS) was prepared using the method first described by Tanev and Pinnavaia [59], and this was combined with a PAN polymer, prepared by in situ polymerization, in the synthesis of a PAN/HMS nanocomposite. The authors chose mercury to examine the prepared nanocomposite's ability to
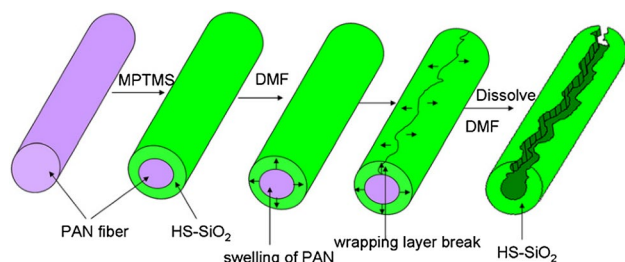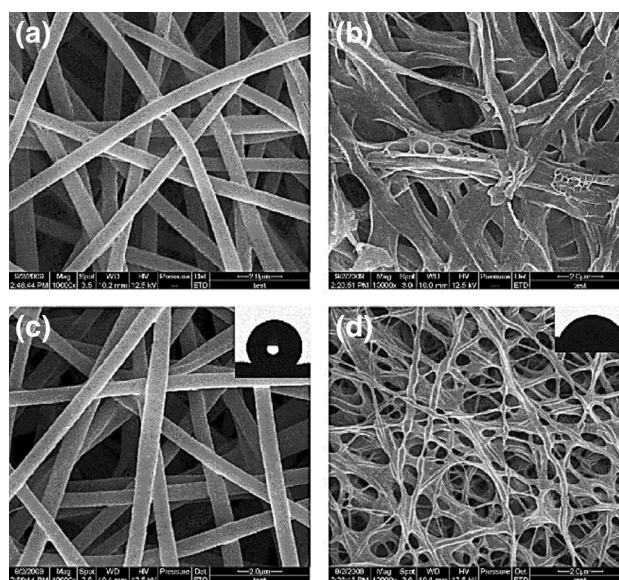

Fig. 6 SEM micrographs of various fibers: **a**, **c** mercaptopropyl silica@PAN fibers before removal of PAN and **b**, **d** zonal mercaptopropyl silica fibers after removal of PAN. The fibers were obtained at the concentrations of MPTS at 180:1:1 (v/v/v) for **a** and **b** and 30:1:1 (v/v/v) for **c** and **d**, respectively. Insets: contact angles of corresponding fibers [58]

take up heavy metal and to establish optimal parameters for its extraction. For this purpose, the pH was optimized and obtained data unsurprisingly revealed that increasing the pH led to the enhancement of the extraction. This reason for this observation is that increasing pH is accompanied by an elimination of the competition between the metal ion and hydronium ion in adsorption on PAN/HMS. The optimal contact time was also determined to be 8 min. Expectedly, the amount of Hg(II) adsorbed on the PAN/HMS nanocomposite correlates strongly with the nanocomposite amount, which was reported to be 800 ppm in this instance. Furthermore, optimizing the initial metal ion concentration showed that higher initial metal concentration results in a decrease in the extraction efficiency. This is mainly due to the confinement of the total existing adsorption sites at high initial concentrations. Additionally, it was seen that by increasing the extraction temperature, adsorptive forces between the active sites of the adsorbents, adsorbate species, and nearby molecules of the adsorbed phase were concomitantly increased with an overall improvement in the extraction efficiency. The reported data also showed more than 88% of desorption and reusability of the adsorbent for three cycles, which makes the nanocomposite suitable one for Hg(II) extraction. Finally, the optimum extraction condition was performed on water samples from wastewater disposals of chlor-alkali (CA) units obtained from a petrochemical industry (Bandar Emam Petrochemical, Iran) from which an appreciable amount of mercury was removed [60].

Fig. 5 Fabrication procedure of zonal mercaptopropyl silica nanofibers obtained by dissolution of the PAN nanofiber templates with DMF [58]

In 2014, Wang et al. prepared a mesoporous nanocomposite using chitosan–poly(vinyl alcohol)/bentonite (CTS–PVA/BT) and studied its adsorption ability with Hg(II), Cu(II), Cd(II), and Pb(II) metal ions [61]. Bentonite is clay with the large surface area, high cation exchange capacity, and negative surface charge, which makes it a good candidate for metal extraction goals. Digital and SEM images of prepared CTS–PVA/BT nanocomposites are shown in Fig. 7.

From their study, the researchers found that many of the interesting characteristics of bentonite (BT) were transferred to the nanocomposite. Some of them included increasing average pore radius size (from 2.4 to 6.9 nm with increasing the BT content from 0 to 50%) or decrease in weight loss in thermogravimetric analysis (TGA) analysis (because BT acts as a heat barrier in nanocomposite structure) [62, 63]. Also, the CTS–PVA/BT nanocomposite showed selective adsorption for Hg(II) compared to Cu(II), Pb(II), and Cd(II). The selectivity of the sorbent in the extraction of Hg(II) was evaluated using the selectivity coefficient (k) using Eq. 1:

$$k = {k_d(\text{Hg})} \big/ {k_d(\text{M})} \tag{1}$$

where $k_d(\text{Hg})$ and $k_d(\text{M})$ represent the distribution coefficients of Hg(II) and another metal M, respectively [64–67]. According to the data reported in Table 2, the

adsorption selectivity for the three left metal ions is as follows: Cu(II) > Pb(II) > Cd(II). It was also observed that increasing the BT content from 0 to 50% led to an initial increase in Hg(II) adsorption followed by a slight decrease. Likewise, the experimental extraction ability was much higher than the total theoretical adsorption capacity of BT and CTS–PVA polymer. It was then suggested that the obvious enhancement of mercury adsorption is related to the presence of BT in the structure of the nanocomposite. Furthermore, several mercury salt solutions with varying pH values were studied and no significant change in metal extraction was detected [61].

In 2014, another composite was prepared by S. K. Singh et al., which displayed an impressive potential to take up mercury. This sorbent was obtained by hydrolysis and dehydroxylation–polymerization of silica precursors within a PVA matrix. They chose Hg(II) to investigate the sorbent's capacity for heavy metal removal as well as the various parameters affecting metal adsorption such as pH, salt effect, adsorbate initial concentration, temperature, and quantity of adsorbent. According to the data obtained from pH drift experiments (pH$_{ZPC}$), the PVA/silica composite was found to have a positive surface at pH < 4.23, a neutral surface at pH = 4.23, and a negative surface in pH > 4.23. Therefore, optimal pH was estimated to be 6.5 wherein the mercury
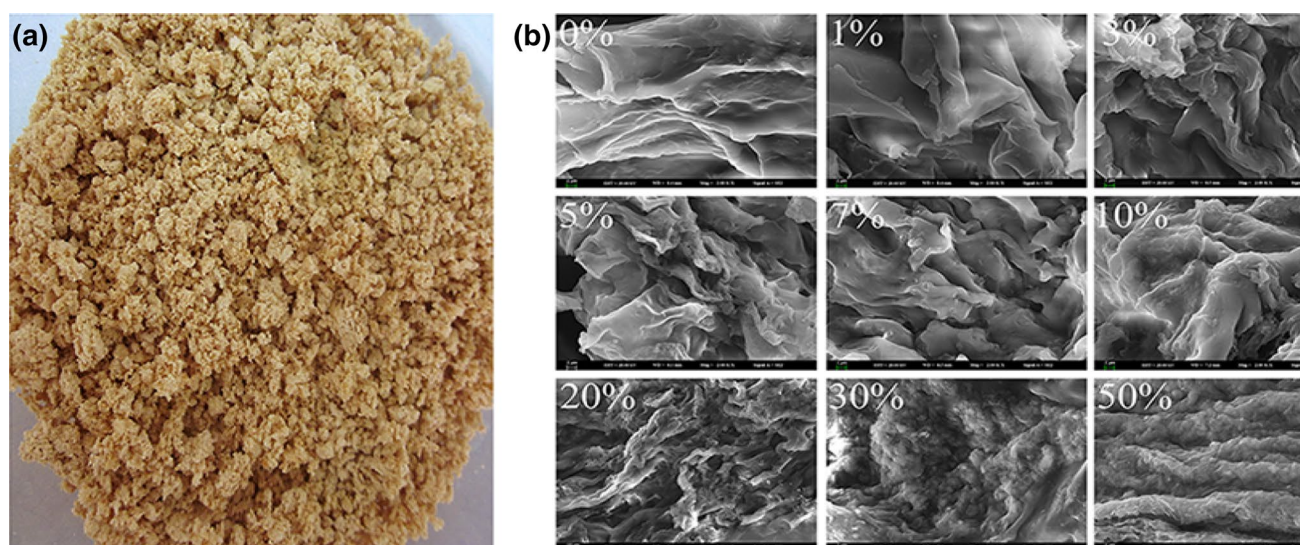

Fig. 7 **a** CTS–PVA/30%BT nanocomposite digital image. **b** CTS–PVA/BT nanocomposites SEM images with various BT contents [61]

Table 2 Selectivity coefficients of the CTS–PVA/BT nanocomposites toward Hg(II) in the presence of other metal species [61]

Metal ions	k				
	CTS–PVA	CTS–PVA/5%BT	CTS–PVA/10%BT	CTS–PVA/30%BT	CTS–PVA/50%BT
Pb(II)	456.25	567.44	586.80	670.86	719.21
Cd(II)	575.11	725.06	734.92	1354.38	1438.42
Cu(II)	1.84	1.56	1.68	1.70	3.65

adsorption was increased from 17.34 to 91.13% with an increase in pH from 1 to 6.5. It was also possible to optimize the adsorbent quantity, and through this, an increase in adsorption was observed up till 50 mg of used adsorbent, which gave a 91% mercury adsorption capability. This increase in adsorption can easily be credited to the enhanced binding sites with increased adsorbents quantity. While optimizing adsorbate concentration, it was observed that increasing the initial mercury concentration resulted in an increase in adsorption. Additionally, enhancement of adsorption was found to accompany increasing extraction temperature from 10 to 30 °C, which proves that Hg(II) adsorption on PVA/silica composite is endothermic in nature. However, the decrease in adsorption at temperatures higher than 30 °C indicates that slight desorption can occur in high temperatures. Interestingly, the ionic strength of the extraction solution was studied in this project. To this end, they used two different salts including NaCl and Na_2SO_4 and investigated their effect on extraction efficiency in various concentration levels. The data clearly indicated that electrolyte ions have an adverse effect on extraction efficiency stemming from the competition in adsorption between Hg(II) and Na^+ ions present in the mentioned salts. Consequently, Na_2SO_4 had a greater influence on the adsorption than NaCl as it contains more sodium ions when compared to the latter [68].

Hierarchical zeolites, which combine both microporosity and mesoporosity, have been synthesized in recent years, to exploit the shape selective properties of microporous zeolites while decreasing the diffusion and accessibility limitations of larger molecules in biomass upgrades [69]. In 2014, Javadian et al. synthesized Beta/MCM-41 hierarchical zeolite and then thiol-functionalized it by post-synthetic grafting using 3-mercaptopropyltrimethoxysilane. Finally, they prepared the polypyrrole/thiol-functionalized Beta/MCM-41 (PPy/SH-Beta/MCM-41) nanocomposite by in situ polymerization method. In studying its Hg(II) adsorption, several parameters including pH, adsorption time, initial concentration, and temperature were optimized. The synthesis pathway of PPy/SH-Beta/MCM-41 nanocomposite and possible Hg(II) adsorption mechanism is shown in Fig. 8. As usual, increasing pH enhanced the adsorption efficiency unless at pH values higher than 8 (because of metal precipitation). The optimal adsorption time was found to be 10 min, which was remarkably shorter than usual optimum contact times. In a bid to justify the short optimum contact time, fast saturation of possible active adsorption sites was suggested. With respect to the endothermic nature of Hg(II) adsorption, an increase in temperature could have both positive and negative impacts on the sorption process. While on the one hand, increasing temperature could enhance adsorption efficiency, on the other hand it could have an inverse effect on desorption. Also, initial metal ion concentration had both beneficial and damaging effects on adsorption
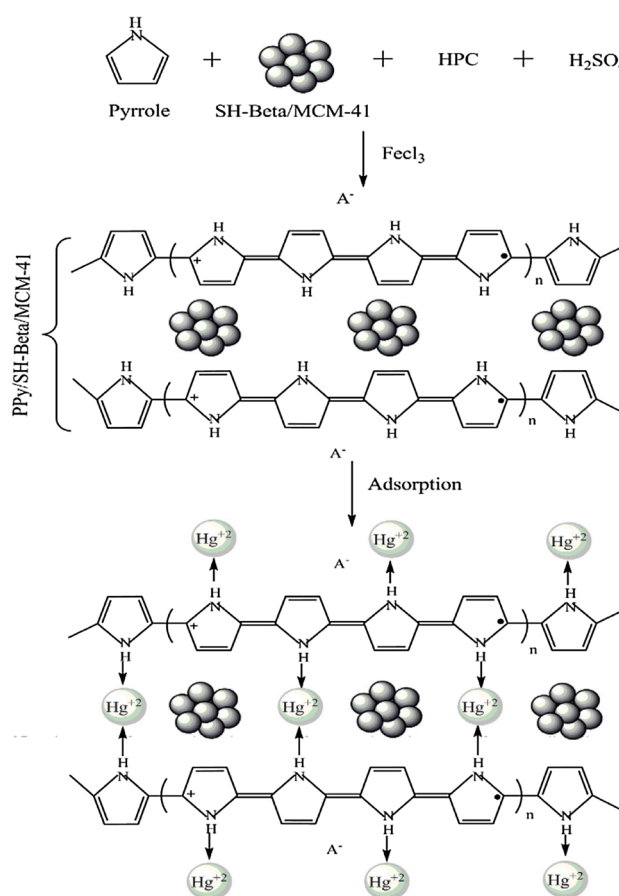

Fig. 8 PPy/SH-Beta/MCM-41 nanocomposite synthesis pathway and the possible mechanism of Hg^{2+} adsorption [70]

and desorption efficiency, respectively. In their desorption studies, they obtained a 90% desorption efficiency using 0.5 M H_2SO_4 solution. Additionally, they reported that the nanocomposite (PPy/SH-Beta/MCM-41) can be used in five adsorption/desorption cycles with little loss in extraction capacity (until 93.5%).

To investigate the applicability of the polymer nanocomposite, they used it to remove Hg(II) in an industrial wastewater sample from a CA Unit from Bandar Emam Petrochemical, Iran. The initial mercury ion concentration was reported 43 mg L^{-1}, and they could remove it using 0.11 g of adsorbent and attained a removal efficiency of 99.52% [70].

Cadmium ion adsorption

Cadmium is an extremely hazardous metal, which has no known necessity in the human body. Cadmium toxicity contributes to a large number of health conditions, including major killer diseases such as cancer, diabetes, and heart diseases [71], when in the body, it can displace zinc, resulting in the latter's deficiency, while also accumulating in the kidney, liver, and other organs. This way it is able to cause

toxicity up to ten times higher when compared to lead and even mercury [72].

In 2009, Singh et al. synthesized a nanocomposite by guar-grafted poly(acrylamide)-templated dehydroxylation polymerization of TEOS [73]. Primarily, the purified guar gum was grafted with poly(acrylamide) (GG-g-PAM). Then, the nanocomposite was prepared using varying ratios of H_2O/TEOS/ethanol (EtOH). The optimal ratio between the three materials was found to be 16:2:1. Finally, the nanocomposites were used for Cd(II) adsorption and the parameters affecting its uptake were optimized. As expected, an increase in adsorbent amount, contact time, agitation speed, and metal ion initial concentration resulted in a higher adsorption efficiency and the optimal value for each parameter was found to be 20 mg, 6 h, 120 rpm, and 500 mg L^{-1}, respectively. In optimizing pH of the adsorption solution, the highest adsorption efficiency was observed at pH = 8. It was then suggested that the surface of the adsorbent has a negative charge and like previously discussed in other studies, low pH values lead to competition between hydronium and cadmium cations. Furthermore, in acidic conditions, Cd(II) forms hydrated species like $Cd(H_2O)_6^{2+}$ and $Cd(H_2O)_4^{2+}$, which cannot pass through nanocomposite pores.

By increasing pH, Cd(II) adsorption on the surface of the nanocomposites improves, but at pH values higher than 9, precipitation of cadmium ion is observed. To this end, pH = 8 was chosen as the optimal pH value. The results obtained from the desorption studies were also quite interesting. Only a slight decrease in adsorption efficiency was observed from the first up to the sixth cycles with a final decrease in removal and desorption efficiency up to 56% and 38%, after the tenth cycle, respectively. This observation supplies good evidence for the adsorbent to have economic advantages [74].

MCM-41 is a remarkable mesoporous silica with uniform honeycomb structure, which has been found to be beneficial in various applications including electronic [75], optics [76], catalysis [77], adsorption [78], and so on. In 2017, two amines modified MCM-41 PNCs using common industrial polymers including poly(methyl methacrylate) (PMMA) (whose modification has been studied in our research team) [79] and polystyrene (PS) were prepared. Primarily, synthesized MCM-41 [80] was modified by (3-triethoxysilyl)-1-propane amine as the silane coupling agent. The modified material was then added to the PMMA and PS polymer solutions and finally, NCs films were formed upon casting. A schematic of APTS–MCM-41/PMMA and APTS–MCM-41/PS is shown in Fig. 9. The modified NH_2–MCM-41/PS and NH_2–MCM-41/PMMA were used for Cd(II) removal, and adsorption parameters including pH, contact time, and metal ion initial concentration were optimized consequently. Stemming from the high concentration of H^+ and its higher mobility toward Cd^{2+} in low pH values, efficient adsorption could not be obtained. However, by increasing pH, the total charge of present functional groups such as hydroxyl and amine was made negative. In addition, at neutral to basic pH hydronium concentration is low compared to the Cd^{2+}. Therefore, optimal pH value and time for highest adsorption efficiency were estimated to be 5.0 and 240 min, respectively, for both modified NCs. Under optimal adsorption conditions, the maximum adsorption capacity for NH_2–MCM-41/PS and NH_2–MCM-41/PMMA was found to be 26.81 mg g^{-1} and 10.59 mg g^{-1}, respectively. Interestingly, it has been observed that the mechanical characteristics of NCs were enhanced compared to the net PMMA and PS [81].

In another study in 2017, we represented a new NC for Cu(II) and Cd(II) adsorption based on aminated MCM-41 and nylon-6 (NY6). NY6 is one of the most important types

Fig. 9 Illustration of MCM-41 surface modification following preparation of APTS–MCM-41/PMMA and APTS–MCM-41/PS NCs for Cd(II) ion adsorption [81]
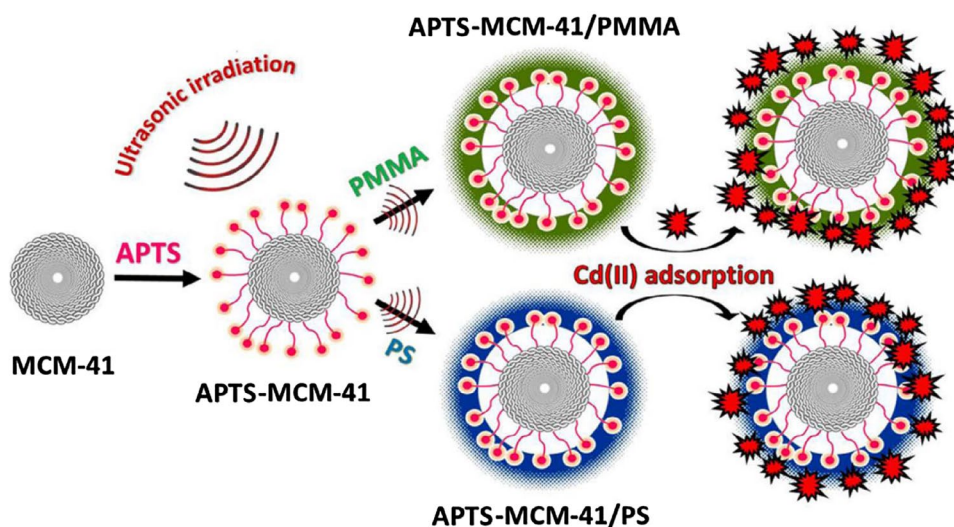
of aliphatic polyamide that has been a subject of great attention in recent years in PNC studies due to their superior film-forming ability, mechanical/chemical properties, and high thermal stabilities [82, 83]. We synthesized MCM-41 and modified it by (3-triethoxysilyl)-1-propane amine. Finally, the modified material was then mixed in NY6 solution and a brittle film was achieved by evaporation of formic acid. The adsorption efficiency of NH_2–MCM-41/NY6 was then examined by the extraction of Cu(II) and Cd(II) as two sample metal ions. The optimal removal conditions were also obtained by studying solution pH, contact time, metal ion initial concentration, and adsorbent dosage. A typical enhancement in metal adsorption by pH increase was observed, and optimum pH values were found to be 6.0 and 5.5 for Cu(II) and Cd(II), respectively. The optimized adsorbent dosage was also estimated to be 25 mg with a maximum adsorption percentage of Cu(II) and Cd(II) to be 99.5% and 76.6%, respectively. It is noticeable that the optimal contact time was reported 75 min for Cu(II) and 90 min for Cd(II), which is somehow faster than other similar studies. This fast metal removal may be attributed to the finite adsorption sites and their availability. Also, it was found that the adsorption capacity of NH_2–MCM-41/NY6 for Cu(II) is spectacularly higher than that of Cd(II). Under optimal extraction conditions, the adsorption capacities for Cu(II) and Cd(II) were found to be 35.8 and 27.6 mg g^{-1}, respectively, which was

asserted to be more efficient in comparison with most adsorbents [84].

In one of the most recent studies on Cd(II) removal, we prepared NCs of an amino-modified MCM-41 and PVA using the ultrasonic-assisted synthetic procedure. A schematic representation of the synthesis procedure is shown in Fig. 10. Adsorption efficiency of the NCs was studied by Cd^{2+} initial concentration and optimized. The expected effect of pH alteration on metal ion adsorption was observed leading to the choice of pH = 6.0 as the optimum pH value. It is noteworthy that under optimal extraction conditions, adsorption capacity of 46.73 mg g^{-1} was achieved, which is acclaimed to be the highest Cd(II) adsorption capability for any silica-based NC reported to date (Table 3). The authors asserted that using ultrasonication during the synthesis procedure led to a fine dispersal of the amine and hydroxyl functional groups within the materials, thereby making them more accessible for metal ions adsorption. This suggests that ultrasonic-assisted NC synthesis may be a good procedure for future metal adsorption studies [85].

Mallakpour et al. have also carried out extensive research on the application of various modified PNCs on Cd(II) removal since 2016. In 2016, they prepared a PNC using PVC as the matrix and modified α-MnO$_2$ with stearic acid (SA) as the nanofiller. The low flammability, low cost, and biological activity of PVC have made it a useful polymer in metal extraction studies [48, 52]. However,
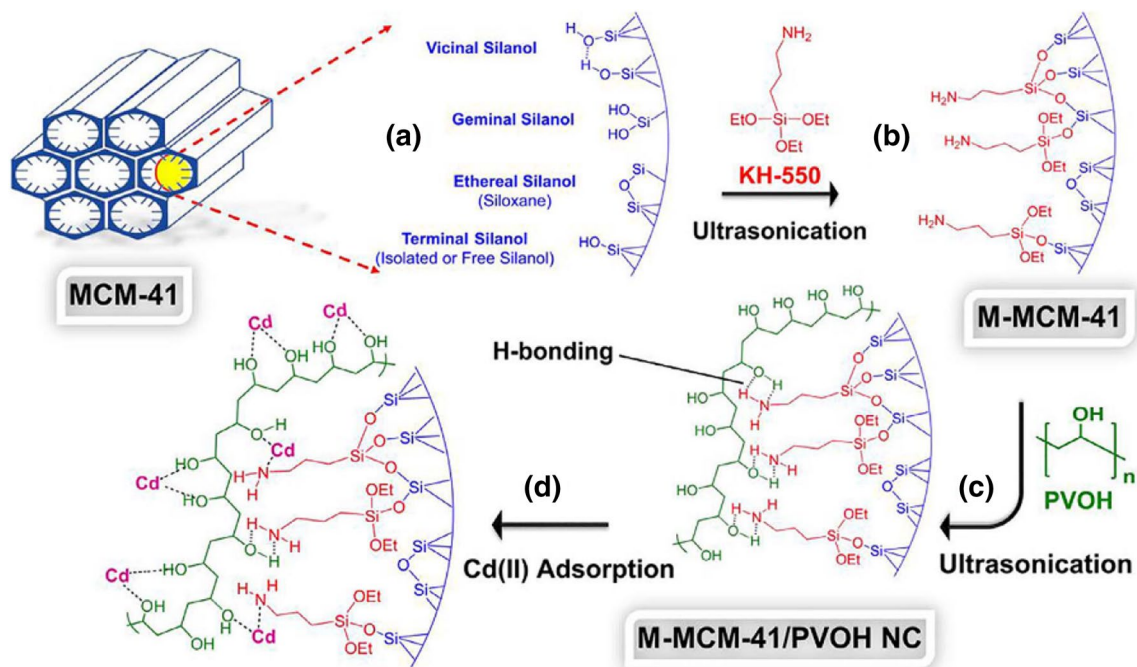

Fig. 10 Schematic illustration for fabrication of the m-MCM-41/PVOH NC for Cd(II) adsorption: a four types of silanol groups on the surface of MCM-41; b surface modification of MCM-41 with KH550 (a silane coupling agent); c preparation of m-MCM-41/PVOH NC via casting solution method with water as solvent; d adsorption of Cd(II) from aqueous media [85]

Table 3 Comparison of the adsorption capacity of m-MCM-41/PVOH NC toward Cd(II) ions with other adsorbents [85]

Adsorbent[a]	Q_m^b(mg g^{-1})	pH	References
M-MCM-41/PVOH NC	46.73	6.0	[85]
NH$_2$–MCM-41/NY6 NC	27.59	5.5	[86]
APTS–MCM-41/PMMA	24.75	5.0	[81]
APTS–MCM-41/PS	10.42	5.0	
NH$_2$–MCM-41	18.25	5.0	[87]
SNHS	20.82	4.5	[88]
Si–NH$_2$	31.89	4.5	
NH$_2$–SNHS	40.73	4.5	
Si–DHB	~3.60	6.0 to 7.5	[89]
Si–DHAQ	~8.10	7.0	[90]
Si–APTS–EDTA	23.67	5.5	[91]
HMS–NH$_2$	28.10	–	[92]
HMS–SH	14.61	–	

Si silica; *DHB* 3,4-dihydroxybenzene; *DHAQ* 1,8-dihydroxyanthraquinone; *APTS* 3-aminopropyltriethoxysilane; *EDTA* ethylenediaminetetraacetic acid; *HMS* hexagonal mesoporous silica

[a]SNHS: silica nano hollow sphere

[b]The maximum adsorption capacity

PVC requires modification due to some of its defects that limit its application such as poor impact toughness and low thermal stability. They have already noticed the special properties of α-MnO$_2$ [47, 49–51]; nevertheless, it needs to be modified to reduce its agglomeration in PNC structure. SA is a saturated fatty acid with a hydrophilic head and a hydrophobic tail, which can act as a surfactant and enable fine dispersal of α-MnO$_2$ nanorods in the polymer chain. They prepared the α-MnO$_2$–SA nanorods via a simple solvothermal process and dispersed it at different amounts in PVC. Eventually, they investigated the Cd(II) removal ability of PVC/α-MnO$_2$–SA NC 5 wt% in 10 mL of neutral metal ion solution at room temperature for 180 min. According to the reported data, the adsorption capacity of PVC/α-MnO$_2$–SA NC is 178.5 mg g^{-1}, which was clearly greater than the value obtained from neat PVC (74.6 mg g^{-1}) [93]. In another study, Mallakpour et al. used PVA instead of SA in order to modify α-MnO$_2$ nanorods surface and observed that PVA could improve miscibility and subsequently enhance the interfacial bonding between the α-MnO$_2$ and PVC matrix. Cd(II) adsorption studies revealed that PVC/α-MnO$_2$–PVA 5 wt% attained a maximum adsorption of 32.6 mg g^{-1} [46]. In 2017, they reported two other studies on SA-modified α-MnO$_2$; in the first one, they used this modified nanofiller in PVA matrix using a green ultrasonic-assisted technique similar to their other studies. Ultrasonication time has also been optimized and 60 min has been chosen, because technically no changes were observed in the

dispersion of modified nanorods with increasing time from 60 to 75 min. Hydroxyl functional groups present on the PVA/α-MnO$_2$–SA nanocomposite that is related to both PVA and the α-MnO$_2$ (Mn–OH) nanofiller enable adsorption of Cd(II) through chelation and ion exchange mechanisms. Adsorption equilibrium was attained in 24 h, which is believed to be the equilibrium state for PVA/α-MnO$_2$–SA NC 5 wt%, with the adsorption capacity of 15.46 mg g^{-1} [94].

PVP has a lactam ring with a proton-accepting carbonyl group, while PVA with its abundant hydroxyl groups can form hydrogen bonds with carbonyl groups. It is thus expected that the introduction of PVP in the PVA–NC can enhance the latter's properties such as adsorption of heavy metals, physical, and thermal properties. Mallakpour et al. used this specific polymer combination while still modifying it with α-MnO$_2$–SA and subsequently utilized it in Cd(II) adsorption studies [95]. The amide and hydroxyl groups in the backbone of the prepared PNC were able to adsorb Cd(II) by chelation and also ion exchange mechanism due to the lone pairs of nitrogen/oxygen atoms and surface Mn–OH groups, respectively. Finally, the 5 wt % blend of PVA/PVP/α-MnO$_2$–SA NC revealed a maximum metal removal capacity of 47 mg g^{-1}, which is about threefold higher than their previous study with PVA/α-MnO$_2$–SA PNC [95].

They have also reported a modification of α-MnO$_2$ with other compounds; for example in 2017, biofunctionalized α-MnO$_2$ nanorods with different amino acids including alanine, leucine, isoleucine, methionine, LVA, and phenylalanine were prepared and characterized by FTIR and XRD techniques. Cd(II) adsorption studies for α-MnO$_2$–LVA in neutral metal solutions exhibited the maximum adsorption capacity of 28.4 mg g^{-1}, which is surprisingly lower than neat α-MnO$_2$ (38.2 mg g^{-1}). However, they claimed that the metal adsorption property of α-MnO$_2$–LVA-modified nanorods is comparable with other PNCs [96].

Layered double hydroxide (LDH) materials are hydrotalcite-type solids with layered structures possessing positive charges balanced by anionic interlayer materials. It is then possible to design a variety of 2D nanosheet materials by simply incorporating various anionic compounds within the expandable interlayer space of LDH. Accessibility, easy and cheap preparation, and high level of anion exchange capacity in the purification of the aqueous solution [97] have made LDH an appropriate material for different applications. Mallakpour et al. prepared and characterized a diacid (having L-phenylalanine segment)-intercalated LDH (I-LDH)/PVC. The structure of LDH is polar and full of electronegative hydroxyl clusters, which can increase positive interaction of this material with the matrix of PVC. According to the observed data, the specific surface area, pore volume, and pore diameter for I-LDH were higher in comparison with those obtained from pure LDH. This was then asserted to be

due to the presence of the organic molecules in the structure of I-LDH, which aided pore expansion resulting in its higher porosity in comparison with the non-modified material. As LDH is unstable in the acidic condition, it was, therefore, necessary to perform a pH adjustment raising it up to a value of 7 during the Cd(II) adsorption studies. They also reported that high pH values were also unfavorable because of Cd(OH)$_2$ precipitation and also LDH capacity reduction due to the high concentration of negatively charged hydroxyl groups. Consequently, 0.10 g of I-LDH/PVC NC 15 wt% in 10 mL of 50 mg L^{-1} of neutral cadmium solution and shaking at room temperature for 120 min has been reported as the optimal conditions Cd(II) extraction. From this, a value of 31.51 mg g^{-1} was determined for the maximum adsorption capacity. The uptake capacity of I-LDH/PVC NCs for cadmium could be seen to correlate with the PVC functional groups [98].

Mallakpour and co-workers also investigated other PNCs potential for Cd(II) removal whose compositions, extraction conditions (they were all performed in pH = 6 and ambient temperature), maximum capacities, and highlights are summarized in Table 4.

Chromium ion adsorption

Chromium is a metal that is usually found in two oxidation states in aqueous solutions; Cr(III) and Cr(VI) with the latter being its most dangerous form due to the serious risks that it can pose to human health. Within the human body, Cr(VI) is reduced to Cr(III), which then forms stable complexes with nucleic acid and proteins. Therefore, Cr(VI) is regarded as a carcinogenic metal as its ingestion can cause skin irritation, lung and kidney cancer, and gastric damage. In fact, chromium contamination is so dangerous that the maximum allowable concentration of Cr(VI) in drinking water is a reported value of 0.05 mg L^{-1} by the WHO [104].

In 2015, Wilson et al. used SBA-15 and modified it with ferulic acid (FA), thereby yielding an adsorbent with high porosity due to the presence of SBA-15 as well as an enhanced hydrophobic surface stemming from the use of FA. The desired nanocomposite was then synthesized by in situ radical polymerizations of vinyl monomers in the presence of FA-functionalized ordered mesoporous silica (SBA/FA). Afterward, the SBA/FA nanocomposite capability as an adsorbent was examined for Cr(VI) extraction. It has been reported that SBA-15 did not show any significant Cr(VI) adsorption and FA has the major function that makes SBA/FA nanocomposite suitable for Cr(VI) adsorption. Various percentages of styrene and FA were used to prepare the nanocomposite, and then, their extraction efficiencies were studied with their best adsorption capacities being obtained with 50% of each. Interestingly, the optimal pH value and contact time were determined to be 4 and 6 h, respectively,

both of which were chosen as optimum extraction conditions. It is also worth mentioning that the SBA/FA nanocomposite could be reused for three cycles with only a 5–8% reduction in adsorption efficiencies [105].

Another heavy metal ion that can be perilous for human health is Cu(II). Excessive intake of this metal ion has been found to result in liver and kidney damage, gastrointestinal problems, nausea, and headaches [106]. In 2015, Chávez-Guajardo et al. prepared maghemite nanoparticles using chemical co-precipitation methods and prepared PPY/γ-Fe2O3 and PANI/γ-Fe2O3 MNCs by emulsion polymerization of pyrrole and aniline, respectively. They used these MNCs for extraction of Cu(II) and Cr(VI) and optimized three parameters effecting extraction efficiency namely—pH, initial heavy metal ion concentration, and contact time. An illustration of their metal extraction process and magnetic behavior is shown in Fig. 11. An important advantage of magnetic adsorbents is their ease of separation via a magnet with suitable power, which allows sufficient separation with no centrifugation step. Table 5 shows the optimized adsorption conditions obtained for the MNCs.

As can be understood from data shown in Table 5, the optimized pH value for Cr(VI) is much lower than those obtained for other similar metal adsorption studies. This observation can be attributed to the use of K$_2$Cr$_2$O$_7$ as the Cr(VI) source in this study, which is known to form various ionic structures depending on the pH. For instance, CrO$_4^{2-}$ is main ion in pH > 6.0, while Cr$_2$O$_7^{2-}$ and HCrO$_4^{-}$ are the dominant species at pH 2.0–6.0 and H$_2$CrO$_4$ at pH < 1.0 [108]. Therefore, in the pH range of this study, Cr(VI) is mostly in either or both of its Cr$_2$O$_7^{2-}$ and HCrO$_4^{-}$ forms. Consequently, a protonated surface at low pH values with good electrostatic interaction to the negative chromate ions can display high adsorption efficiency. Also, it has been found that at low pH values, PANI undergoes oxidation while Cr(VI) is reduced to Cr(III), thus allowing the formation of chelates that can aid Cr(VI) extraction. But for Cu(II) ion, the usual pH effect is observed and pH values higher than 5.5 were not discussed due to the precipitation of Cu(II) in pH > 5.5. Concerning the reusability of the adsorbents, both of them showed good performance over four cycles, except for PANI/γ-Fe$_2$O$_3$ with respect to Cu(II) removal whose adsorption dropped to 84% after three cycles [107].

In one of the most recent studies on Cr(VI) adsorption, we prepared a series of novel, modified mesoporous silica MCM-41/polymer matrix nanocomposites. MCM-41 and its (3-aminopropyl)triethoxysilane-modified form were synthesized and then 2 wt% of the modified NCs in PVA, PS, NY6, and PMMA polymer solutions were prepared via sonication (Fig. 12).

The prepared PNCs were also characterized by XRD, FTIR, SEM, and TEM techniques, while their adsorption efficiencies were studied using Cr(VI) as the target metal

Table 4 Summary of some recent studies on Cd(II) adsorption

PNC (adsorbent)	Filler (wt%)	Adsorption condition		Q_m (mg g^{-1})	Highlights	References
		t (h)	Stirring speed (rpm)			
PVA/CaCO$_3$–DA*	3, 5, 8	3	150	PNC 5 (wt%) = 20.70	Bioactive DA has enhanced CaCO$_3$ surface from hydrophobic to hydrophilic	
				PNC 8 (wt%) = 25.19	Cd(II) is adsorbed through complexation mechanism	[99]
rPET/MWCNT–ZnO QD**	1, 2, 4	3	180	rPET = 35	The PNC is a combination of zero-dimensional (0D) QDs and one-dimensional (1D) CNTs	[100]
				rPET/f-MWCNT = 13		
				PNC 4 (wt%) = 56	Cd(II) metal ion is adsorbed by –OH, –COOH and –C=O functional groups	
Chit/starch–MWCNT–LVA (CSMV)	30, 50, 70	1.5	150	CSMV 70 (wt%) = 16.63	Ambient presence of hydroxyl and carboxylic functional groups on CSMV surface and thus effective metal extraction ability is obtained	[101]
rPET/MWCNT–LDH	1, 2, 4	12	170	rPET = 11.35	The pH$_{PZC}$ was found to be 7 and in pH < pHPZC, the PNC's surface is protonated and has low metal adsorption ability, but in pH > pHPZC PNC's surface is negatively charged	[102]
					Increased ionic strength has improved Cd(II) adsorption, due to dissociation promotion of functional groups by salt	
				PNC 4 (wt%) = 38.91	PNC has shown high selective removal efficiency toward Cd(II) among Ni(II) and Pb(II) metals	
					Two pathways were suggested for Cd(II) removal: 1) inner complexation of metal with –OH and –COOH (mono- and bidentate), 2) outer complexation (main pathway)	
					PNC can be used for three adsorption cycles.	
rPET/CMWCNT***	1, 2, 4	17	Not mentioned	rPET = 10	The electrical conductivity of PNC has been greatly enhanced (at a concentration of only 1 wt% PNC electrical conductivity increased by nine orders of magnitude compared to that of the pure PET)	[103]
				PNC 2 (wt%) = 22		

* Diacid

**Quantum dot

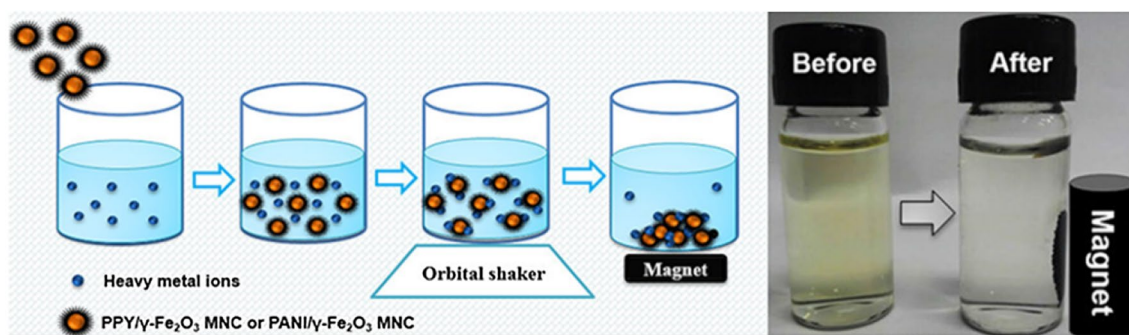***Recycled PET/carboxylated multi-walled carbon nanotube composite

Fig. 11 Extraction process and magnetic behavior of PPY/γ-Fe$_2$O$_3$ and PANI/γ-Fe$_2$O$_3$ PMNCs [107]

Table 5 Optimized adsorption condition obtained for PPY/γ-Fe$_2$O$_3$ and PANI/γ-Fe$_2$O$_3$ [107]

Parameter	PH		The initial metal ion concentration		Contact time (min)	
Heavy metal ion	Cr(VI)	Cu(II)	Cr(VI)	Cu(II)	Cr(VI)	Cu(II)
PPY/γ-Fe$_2$O$_3$	2.0	5.5	Above 75 mg L^{-1}	15^a	15^b	
PANI/γ-Fe$_2$O$_3$	2.0	5.5			15	15

^{a}PPY/γ-Fe$_2$O$_3$ adsorbs Cr(IV) faster than PANI/γ-Fe$_2$O$_3$; in fact, it can adsorb 50% of Cr(IV) in 5 min

^{b}PPY/γ-Fe$_2$O$_3$ adsorbs Cu(II) faster than PANI/γ-Fe$_2$O$_3$, but its adsorption speed is less than Cr(IV) adsorption
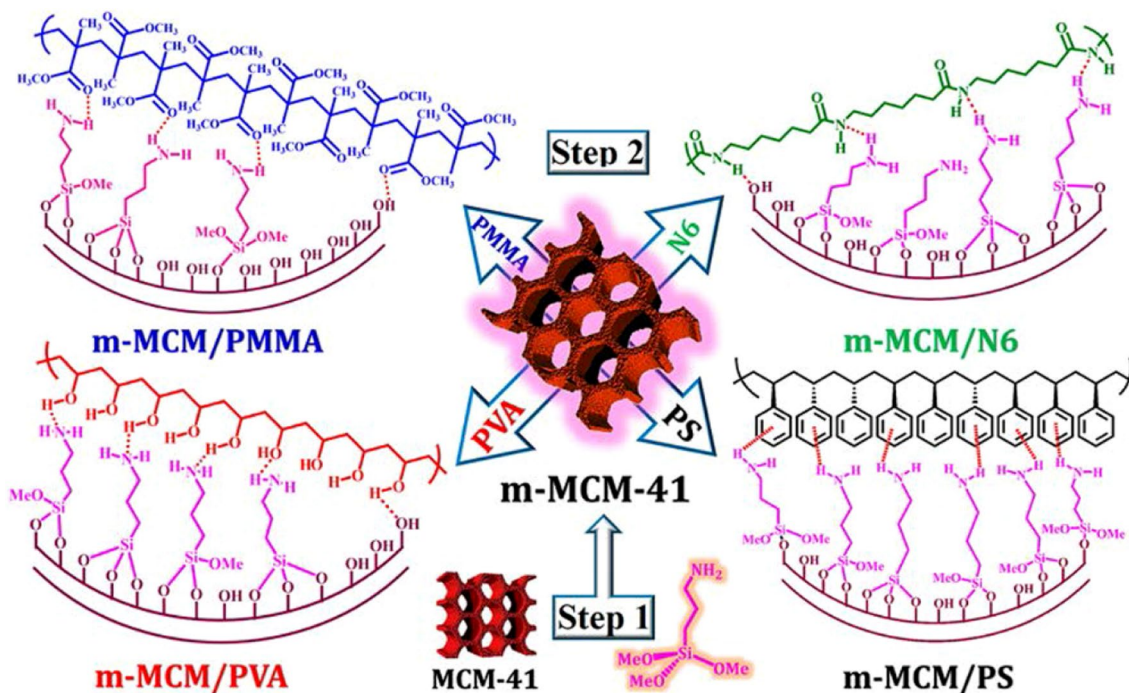

Fig. 12 Schematic illustration of the m-MCM-41/polymer matrix nanocomposites (PMNCs) formation: (step 1) preparation of m-MCM-41 by silane modification of MCM-41 pristine; (step 2) m-MCM-41/PMNCs formation [109]

ion. As usual, solution pH was optimized and instead an inverse relationship between pH and adsorption efficiency was observed, which runs contrary to the normal trend.

As shown in Fig. 13, there is a sudden increase in Cr(VI) removal in the pH range of 1–2. However, at pH values higher than 2, all four NCs showed a decrease in adsorption
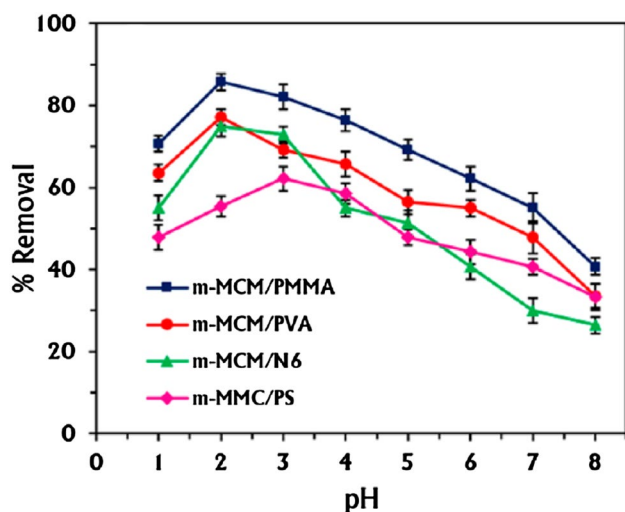
Fig. 13 Effect of solution pH values on Cr(VI) removal percentage by m-MCM-41/NCs [109]

Fig. 14 PANI/HMS synthesis pathway [111]

leading to the choice of 2 as to be optimum for metal adsorption study. This behavior was adduced to the pH variation in the forms, which Cr(VI) can adopt in solution, in particular, its occurrence as $Cr_2O_7^{2-}$, $HCrO_4^-$, CrO_4^{2-} and $Cr_3O_{10}^{2-}$ at low pH and mainly $HCrO_4^-$ at pH range 2–5. At a pH greater than 5.5, the main form of Cr(VI) becomes the CrO_4^{2-} ion. As it is expected that at low pH values, the existing functional groups on the surface of NCs such as hydroxyl, ketone, amine, and phenyl tend to be protonated—OH_2^+, $-C=OH^+$, $-NH_2^+$, and $-NH_3^+$. These are unsurprisingly perfect for adsorption of Cr(VI) stemming from the ease of interaction of these oppositely charged species with each other. Therefore, any increase in the pH should result in the positive charges of functional groups becoming negative, thereby leading to the observed decrease in Cr(VI) removal for all of the aforementioned NCs. Contact time and Cr(VI) initial concentration were also optimized, and adsorption capacity of 20, 18.5, 17.9, and 15 mg g^{-1} was reported for m-MCM-41/PMMA, m-MCM-41/PVA, m-MCM-41/NY6, and m-MCM-41/PS, respectively. The removal efficiency of Cr(VI) was found to be in the range of 61.78–85.71%, but unfortunately, the reusability of prepared PNCs was not investigated in this study [109].

Other metals

Nickel is one of the heavy metals that play an important role in the human body including ureolysis, hydrogen metabolism, methane biogenesis, and acidogenesis [110]. If the Ni level in the human body exceeds its beneficial value, it can cause diseases such as skin dermatitis, lung cancer, gastrointestinal disorder, and renal edema. In order to remove this heavy metal from aqueous real samples, Javadian et al.
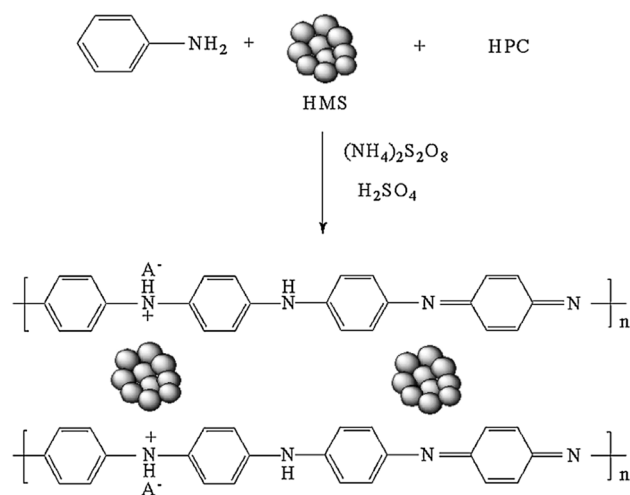
suggested a nanocomposite prepared from PANI and HMS. They synthesized the PANI/HMS nanocomposite by in situ chemical polymerization process by utilization of ammonium peroxodisulfate (APS) as an oxidant (a schematic of PANI/HMS preparation is shown in Fig. 14) and studied its adsorption ability for removing Ni(II) from aqueous solutions as a heavy metal model sample. Interestingly, the optimum pH for this adsorption was 8, which is similar to the adsorbent prepared by Singh et al. [74]. The optimum pH has been attributed to the Ni oxidation state and the behavior of functional groups present in the PANI/HMS NCs in the pH range of 2–8. Under acidic conditions, nitrogen (N) containing groups become protonated and can no longer adsorb the metal cation sufficiently. Working under alkaline conditions, however, results in the polymer transforming into its deprotonated emeraldine base, thereby leading to the amine or imine groups in the polymer being available for metal chelating, which is accompanied by increased Ni(II) sorption. Other extraction parameters including contact time, adsorbent dosage, solution volume, and metal initial concentration were likewise optimized, and a trend similar to other studies was observed. Finally, an extraction condition with 0.05 g of PANI/HMS nanocomposite in a 50 mL of Ni(II) aqueous solution with pH = 8 for 16 min was reported as the optimal condition. Also, 0.1 M H_2SO_4 was utilized for Ni(II) desorption from the PANI/HMS, which showed 86% of maximum desorption efficiency. The recycled sample shows substantial removal efficiency with less than 10% reduction. Finally, a real sample from wastewater disposals of plating manufactory, Isfahan, Iran, was extracted using the nanocomposite and good performance was observed [111].

In 2015, an interesting study was done by Borai et al., which focuses on three rare heavy metals including cesium

(Cs(I)), cobalt (Co(II)), and europium (Eu(III)) that all have different charges and radiuses. For this purpose, they prepared two nanocomposites, one of which is the TiO_2/poly (acrylamide–styrene sodium sulfonate) [TiO_2/ (P(AAm–SSS))] prepared by in situ intercalative polymerization of poly(acrylamide) (PAAm) and styrene sodium sulfonate (SSS) in the presence of TiO_2 nanoparticles as inorganic filler. In this polymerization, γ-radiation and N-methylenebisacrylamide (MBA) were used as reaction initiator and cross-linker, respectively. The second nanocomposite was PS/TiO_2 that was prepared by the ionic polymerization method. The prepared NCs were used for adsorption of the aforementioned metal ions after their characterization by XRD, TGA, FTIR, etc. Increasing the pH values had an expectedly positive effect on adsorption with maximum removal obtained at pH 5, 6, and 8 for Eu^{3+}, Co^{2+}, and Cs^+, respectively. It was also revealed that the TiO_2 content played an important role in removal efficiency, i.e., a decrease in adsorption was observed in more or less than 0.06 g of TiO_2. Upon decreasing the nanoparticle concentration, an increase in the water-soluble fragment of the nanocomposite was expected, which resulted in lower Co^{2+} and Eu^{3+} removal. For higher concentration of nanoparticles (> 0.06 g), the density of cross-linking in the NC was considerably increased. Consequently, a decrease in accessible structural network spaces led to less adsorption of Co^{2+} and Eu^{3+}. PS–TiO_2 and TiO_2 nanoparticles showed similar trends in the optimization of shaking time that could be related to either PS degradation at high temperature or the coverage of PS functional group by TiO_2, which impedes the removal process. The maximum adsorption capacities were reported as 120, 100.9, and 85.7 mg g^{-1} for Cs^+, Co^{2+}, and Eu^{3+}, respectively. Cs(I), unsurprisingly, had the highest adsorption capacity because of its small hydrated radius and high electropositivity compared to the other two metal ions [112].

Copper accumulation in living organisms over time can cause serious gastrointestinal problems, kidney and liver damage, headaches, and nausea, which made EPA announce the maximum safe Cu(II) concentration limit in drinking water to be 1.3 mg L^{-1} [113]. Therefore, Cu(II) can be a good target compound to be adsorbed using PNCs. Nanoboehmite with remarkable characteristics has already been a material of interest in our studies for the preparation of modified boehmite (mB)–PA6 NCs [114]. It can be also merged with PMMA, which is a hydrophilic polymer, to prepare a good candidate for Cu(II) extraction [115]. Fascinating properties of silane-modified nano-boehmite with hydrophilic polymers such as high surface area have been studied previously [114]. We used this combination while enhancing nano-boehmite properties by silane coupling agents. According to FE-SEM characterizations, the AlOOH flake-like morphology underwent a change to a spherical

form after modification, which was also preserved in the corresponding NC. Finally, the resultant PMMA/m-AlOOH NC with 1, 2, and 3% of modified filler was obtained using an in situ polymerization technique. Cu(II) adsorption capacities of aforementioned PNCs were investigated by introducing 10 mg of modified nano-boehmite and PMMA (MBNCs) to 10 ppm solution of Cu(II) while shaking at 150 rpm at room temperature. Two important adsorption factors including pH and adsorption time were also optimized. As it was expected, higher pH is favorable due to less competition between H$^+$ and the target analyte. Additionally, higher pH values allow the existence of abundant hydroxyl functional groups on modified nano-boehmite. It was found that the nanocomposite with 3% of modified boehmite displayed Cu(II) adsorption greater than 94% (120 min and pH = 4.0), indicating that the material would be a good fit for use in copper removal. A schematic of Cu(II) adsorption by PMMA/m-AlOOH NC is shown in Fig. 15 [115].

Recently, we have also report the synthesis and characterization of m-MCM-41/PMMA nanocomposites [116]. In this study, MCM-41 was synthesized and then functionalized using 3-aminopropyl triethoxysilane. In the following, m-MCM-41/PMMA nanocomposites were prepared through in situ polymerization with different weight percentages of m-MCM-41 (1, 2, and 4 wt%). The prepared PMNCs showed a good thermal stability, but the 2% PMNC was chosen overall after various characterizations and used for adsorption studies of Cu^{2+}. Langmuir isotherm model suggested to be well fitted with the experimental data and the maximum value of adsorption capacity toward copper(II) ions was found to be 41.5 mg g^{-1} (pH = 4, adsorbent dose 10 mg, temperature 25 °C, stirring speed 180 rpm, and time 140 min).

Mallakpour et al. have also performed Cu(II) adsorption experiments on PNCs with diverse chemical compositions since 2017. The highlights of their studies are summarized in Table 6.

Conclusion

In this review, we have tried to abridge PNCs metal adsorption studies with an emphasis on their special highlights. As already mentioned, nanofillers are a group of valuable materials, whose fascinating properties can be reinforced when combined with polymers. Since nanofillers are mostly inorganic materials, they need to be modified by a surfactant, thus reducing the possibility of agglomeration while enhancing the adsorption properties of their corresponding PNC. Although the porosity of PNCs can have a direct effect on its adsorption efficiency, their chemical structures and functional groups should be considered carefully for compatibility with the chemical
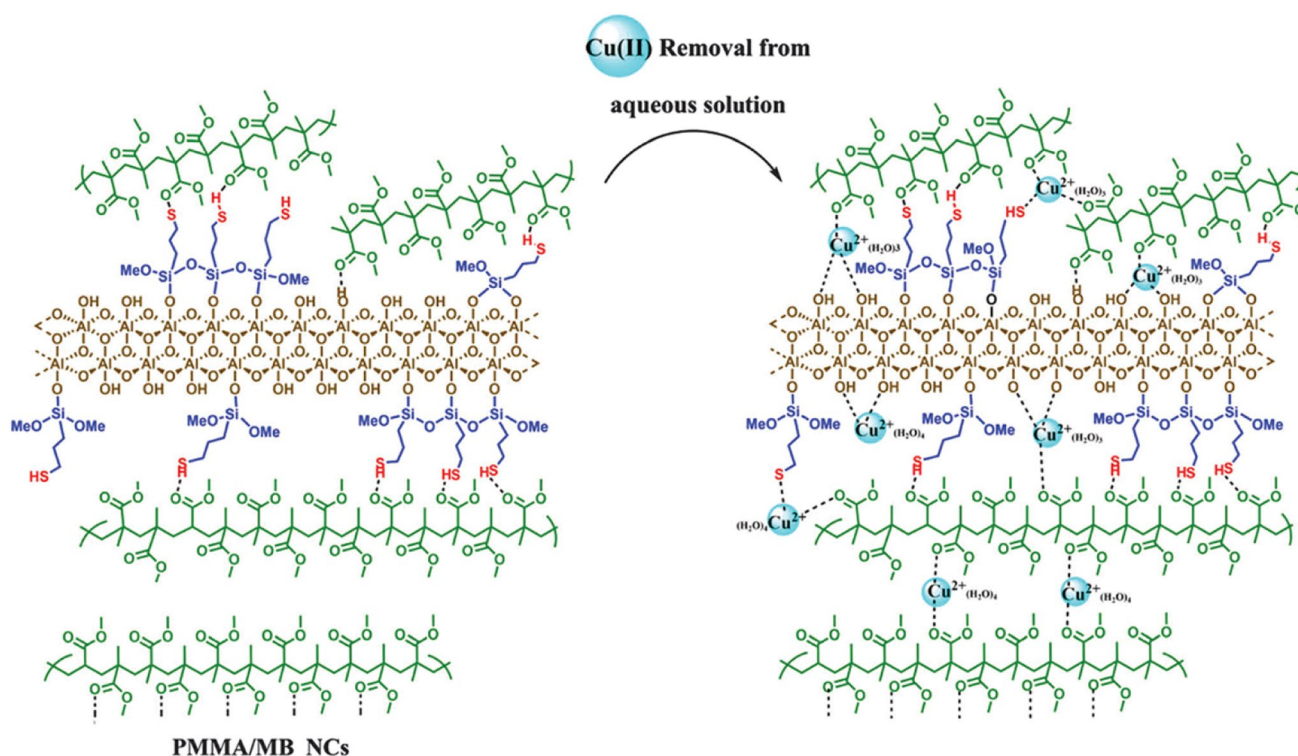
Fig. 15 Schematic representation of Cu(II) removal by MB/PMMA hybrids [115]. Reproduced by permission of the royal society of chemistry (RSC) on behalf of the Centre National de la Recherche Scientifique (CNRS) and the RSC

Table 6 Summary of some recent studies on Cu(II) adsorption

PNC (adsorbent)	Time (h)	Q_m (mg g^{-1})	Highlights	References
PVA/CaCO$_3$–KH550	3	PVA = 21.32	Metal adsorption was performed in pH = 6.5	[117]
			Formation of hydrogen bonds and van der Waals forces between ATS amino and PVA (–OH) groups prevents agglomeration	
		PNC 5 (wt%) = 45.45	High removal efficiency is due to the coordination interaction between Cu2 + and –OH, –C=O and –NH2 functional groups	
CS/CaCO$_3$–DA	3	PNC 5 (wt%) for Cu(II) = 21.74	L-phenyl aniline (2–8 wt%) was used as DA.	[118]
			Adsorption experiments were carried out for both Cu(II) and Cd(II)	
		PNC 5 (wt%) for Cd(II) = 29.41	Both metals were adsorbed by PNC through complexation with oxygen and nitrogen present in functional groups on the PNC's surface	
			PNC has shown a great tendency toward Cu(II) compared to Cd(II) because: a) Cu(II) has higher electronegativity than Cd(II). b) Oxygen in filler's functional groups is known as a hard base which mostly adsorbs the harder metal (Cu(II))	
Starch/MWCNT–LVA	0.5	Not reported (removal efficiency = 66% in optimum condition)	The most prevalent interaction between starch and MWCNT–LVA is hydrogen bonding	[119]
			Short adsorption time equilibrium is due to a large number of unoccupied surface sites	
			Cu(II) adsorption was performed through chelation (considering amide and carboxylic acid as chelating agents)	

Table 7 Summary of PNCs with highest adsorption efficiency for heavy metal removal

Metal Ion	PNC	Q_m (mg g^{-1})	References
Hg	PAN/HMS	843	[60]
Cd	GG-g-PAM–silica	2000	[74]
Cr	PPY/γ-Fe$_2$O$_3$	209	[107]
Cs	TiO$_2$/P(AAm–SSS)	120	[112]
Eu	TiO$_2$/P(AAm–SSS)	85.7	[112]
Co	TiO$_2$/P(AAm–SSS)	100.9	[112]
Ni	PANI/HMS	253.17	[111]
Pb	ALG–SBA-15	222.22	[15]
Cu	PVA/CC–ATS	45.45	[117]

properties of the target metal. Moreover, metal extraction conditions can dramatically effect adsorption efficiency; for example, adsorbent amount, extraction time, pH, ionic strength, temperature, and concentration of metal solution are some of the parameters that should be optimized and accurately controlled. In all of the studies described in this review, the PNCs with highest adsorption capacity (Q_m) for each metal are shown in Table 7, thus revealing the most efficient PNC for the removal of hazardous heavy metals. In spite of the fascinating data obtained from the metal adsorption studies performed until date, the hunt for new and more efficient adsorbents continues.

References

1. M. Jamil, M.S. Zia, M. Qasim, Contamination of agro-eco-system and human health hazards from wastewater used for irrigation. J. Chem. Soc. Pak. **32**, 370–378 (2010)
2. S. Khan, Q. Cao, Y. Zheng, Y. Huang, Y. Zhu, Health risks of heavy metals in contaminated soils and food crops irrigated with wastewater in Beijing, China. Environ. Pollut. **152**, 686–692 (2008)
3. A. Singh, R.K. Sharma, M. Agrawal, F.M. Marshall, Health risk assessment of heavy metals via dietary intake of foodstuffs from the wastewater irrigated site of a dry tropical area of India. Food Chem. Toxicol. **48**, 611–619 (2010)
4. S.-H. Peng, W.-X. Wang, X. Li, Y.-F. Yen, Metal partitioning in river sediments measured by sequential extraction and biomimetic approaches. Chemosphere **57**, 839–851 (2004)
5. F. Fu, Q. Wang, Removal of heavy metal ions from wastewaters: a review. J. Environ. Manage. **92**, 407–418 (2011)
6. Y.-H. Wang, S.-H. Lin, R.-S. Juang, Removal of heavy metal ions from aqueous solutions using various low-cost adsorbents. J. Hazard. Mater. **102**, 291–302 (2003)
7. D.W. O'Connell, C. Birkinshaw, T.F. O'Dwyer, Heavy metal adsorbents prepared from the modification of cellulose: a review. Bioresour. Technol. **99**, 6709–6724 (2008)
8. H. Zou, S. Wu, J. Shen, Polymer/silica nanocomposites: preparation, characterization, properties, and applications. Chem. Rev. **108**, 3893–3957 (2008)
9. L. Wei, T. Tang, B. Huang, Synthesis and characterization of polyethylene/clay–silica nanocomposites: a montmorillonite/silica-hybrid-supported catalyst and in situ polymerization. J. Polym. Sci., Part A Polym. Chem. **42**, 941–949 (2004)
10. J.E. Mark, Some novel polymeric nanocomposites. Acc. Chem. Res. **39**, 881–888 (2006)
11. M. Moniruzzaman, K.I. Winey, Polymer nanocomposites containing carbon nanotubes. Macromolecules **39**, 5194–5205 (2006)
12. N. Bektaş, S. Kara, Removal of lead from aqueous solutions by natural clinoptilolite: equilibrium and kinetic studies. Sep. Purif. Technol. **39**, 189–200 (2004)
13. S. Mallakpour, M. Dinari, G. Mohammadnezhad, Ultrasonic assisted organo-modification of mesoporous SBA-15 with N-trimellitylimido-L-methionine and preparation of the poly (amide–imide)/SBA nanocomposites. Prog. Org. Coat. **78**, 300–306 (2015)
14. M. Dinari, S. Mallakpour, G. Mohammadnezhad, Organo-modification of mesoporous SBA-15 with chiral diacid and its utilization for the preparation of L-phenylalanine-based poly (amide-imide) nanocomposites. Polym. Plast. Technol. Eng. **54**, 549–555 (2015)
15. R. Cheraghali, H. Tavakoli, H. Sepehrian, Preparation, characterization and lead sorption performance of alginate-SBA-15 composite as a novel adsorbent. Sci. Iran **20**, 1028–1034 (2013)
16. J. Wang, X. Li, Synthesis of polyacrylamide/modified silica composite hydrogels for synergistic complexation of heavy metal ions. Desalination Water Treat **53**, 230–237 (2015)
17. J. Wang, F. Liu, J. Wei, Enhanced adsorption properties of interpenetrating polymer network hydrogels for heavy metal ion removal. Polym. Bull. **67**, 1709 (2011)
18. A. Kriger, B. Moyer, S. Alexandratos, Synergistic complexation of metal ions with bifunctional interpenetrating polymer networks. React. Polym. **24**, 35–39 (1994)
19. L. Jiang, P. Liu, S. Zhao, Magnetic ATP/FA/Poly (AA-co-AM) ternary nanocomposite microgel as selective adsorbent for removal of heavy metals from wastewater. Colloids Surf. A Physicochem. Eng. Asp. **470**, 31–38 (2015)
20. Q. Zhao, L. Ren, H. Zhou, T. Cao, P. Chen, Enhanced adsorption of Pb(II) by Al (OH)$_3$/(PAA-CO-PAM) sub-microspheres with three-dimensional interpenetrating network structure. Chem. Eng. J. **250**, 6–13 (2014)
21. Y. Zheng, P. Li, J. Zhang, A. Wang, Study on superabsorbent composite XVI. Synthesis, characterization and swelling behaviors of poly (sodium acrylate)/vermiculite superabsorbent composites. Eur. Polym. J. **43**, 1691–1698 (2007)
22. Y. Zheng, Y. Liu, A. Wang, Fast removal of ammonium ion using a hydrogel optimized with response surface methodology. Chem. Eng. J. **171**, 1201–1208 (2011)
23. Y. Zhao, Y. Chen, M. Li, S. Zhou, A. Xue, W. Xing, Adsorption of Hg^{2+} from aqueous solution onto polyacrylamide/attapulgite. J. Hazard. Mater. **171**, 640–646 (2009)
24. M.-C. van Severen, J.-P. Piquemal, O. Parisel, Enforcing hemi-directionality in Pb(II) complexes: the importance of anionic ligands. Chem. Phys. Lett. **510**, 27–30 (2011)
25. O. Moradi, B. Mirza, M. Norouzi, A. Fakhri, Removal of Co (II), Cu (II) and Pb(II) ions by polymer based 2-hydroxyethyl methacrylate: thermodynamics and desorption studies. Iran. J Environ Health Sci. Eng. **9**, 31 (2012)
26. P. Liu, L. Jiang, L. Zhu, J. Guo, A. Wang, Synthesis of covalently crosslinked attapulgite/poly (acrylic acid-co-acrylamide) nanocomposite hydrogels and their evaluation as adsorbent for heavy metal ions. Ind. Eng. Chem. **23**, 188–193 (2015)
27. S.H. Gehrke, M. Palasis, M.K. Akhtar, Effect of synthesis conditions on properties of poly (N-isopropylacrylamide) gels. Polym. Int. **29**, 29–36 (1992)

28. P. Liu, L. Jiang, L. Zhu, A. Wang, Novel approach for attapulgite/poly (acrylic acid)(ATP/PAA) nanocomposite microgels as selective adsorbent for Pb(II) ion. React. Funct. Polym. **74**, 72–80 (2014)

29. E. Orozco-Guareño, F. Santiago-Gutiérrez, J.L. Morán-Quiroz, S.L. Hernandez-Olmos, V. Soto, W. De la Cruz, S. Gomez-Salazar, Removal of Cu (II) ions from aqueous streams using poly (acrylic acid-co-acrylamide) hydrogels. J. Colloid Interface Sci. **349**(2), 583–593 (2010)

30. M.A. Khan, A. Ahmad, K. Umar, S.A. Nabi, Synthesis, characterization, and biological applications of nanocomposites for the removal of heavy metals and dyes. Ind. Eng. Chem. Res. **54**, 76–82 (2014)

31. A.Z.M. Badruddoza, Z.B.Z. Shawon, W.J.D. Tay, K. Hidajat, M.S. Uddin, Fe3O4/cyclodextrin polymer nanocomposites for selective heavy metals removal from industrial wastewater. Carbohydr. Polym. **91**, 322–332 (2013)

32. S. Singh, K. Barick, D. Bahadur, Surface engineered magnetic nanoparticles for removal of toxic metal ions and bacterial pathogens. J. Hazard. Mater. **192**, 1539–1547 (2011)

33. C.W. Lim, K. Song, S.H. Kim, Synthesis of PPy/silica nanocomposites with cratered surfaces and their application in heavy metal extraction. Ind. Eng. Chem. **18**, 24–28 (2012)

34. A. Liu, K. Hidajat, S. Kawi, D. Zhao, A new class of hybrid mesoporous materials with functionalized organic monolayers for selective adsorption of heavy metal ions. Chem. Commun. **13**, 1145–1146 (2000)

35. M.J. Choi, M.Y. Kim, S.-K. Chang, A new Hg^{2+}-selective chromoionophore based on calix [4] arenediazacrown etherDedicated to Professor Iwhan Cho on the occasion of his 65th birthday. Chem. Commun. **17**, 1664–1665 (2001)

36. A. Suman, M. Kardam, V. Gera, Jain, A novel reusable nanocomposite for complete removal of dyes, heavy metals and microbial load from water based on nanocellulose and silver nano-embedded pebbles. Environ. Technol. **36**, 706–714 (2015)

37. M. Ioelovich, Optimal conditions for isolation of nanocrystalline cellulose particles. J. Nanosci. Nanotechnol. **2**, 9–13 (2012)

38. A. Sato, R. Wang, H. Ma, B.S. Hsiao, B. Chu, Novel nanofibrous scaffolds for water filtration with bacteria and virus removal capability. J. Electron Microsc. **60**, 201–209 (2011)

39. H. Ma, C. Burger, B.S. Hsiao, B. Chu, Ultra-fine cellulose nanofibers: new nano-scale materials for water purification. J. Mater. Chem. **21**, 7507–7510 (2011)

40. D.S. Rajawat, A. Kardam, S. Srivastava, S.P. Satsangee, Nanocellulosic fiber-modified carbon paste electrode for ultra trace determination of Cd (II) and Pb(II) in aqueous solution. Environ. Sci. Pollut. Res. Int. **20**, 3068–3076 (2013)

41. M. Iqbal, A. Saeed, N. Akhtar, Petiolar felt-sheath of palm: a new biosorbent for the removal of heavy metals from contaminated water. Bioresour. Technol. **81**, 151–153 (2002)

42. P. Goyal, P. Sharma, S. Srivastava, M. Srivastava, Saraca indica leaf powder for decontamination of Pb: removal, recovery, adsorbent characterization and equilibrium modeling. Int J Environ Sci Technol (Tehran) **5**, 27–34 (2008)

43. S. Devaraj, Studies Of MnO_2 As Active Material For Electrochemical Supercapacitors, G23079, 2010

44. D.N. Thanh, M. Singh, P. Ulbrich, F. Štěpánek, N. Strnadová, As (V) removal from aqueous media using α-MnO_2 nanorods-impregnated laterite composite adsorbents. Mater. Res. Bull. **47**, 42–50 (2012)

45. P.-Y. Kuang, M.-H. Liang, W.-Y. Kong, Z.-Q. Liu, Y.-P. Guo, H.-J. Wang, N. Li, Y.-Z. Su, S. Chen, Anion-assisted one-pot synthesis of 1D magnetic α-and β-MnO_2 nanostructures for recyclable water treatment application. New J. Chem. **39**, 2497–2505 (2015)

46. S. Mallakpour, A. Abdolmaleki, H. Tabebordbar, Facile synthetic route for the preparation of PVC/α-MnO2-PVA nanocomposites: morphology, thermal, mechanical and Cd (II) adsorption properties. Polym. Bull. **74**, 2957–2973 (2017)

47. S. Mallakpour, M. Madani, Functionalized-MnO2/chitosan nanocomposites: a promising adsorbent for the removal of lead ions. Carbohydr. Polym. **147**, 53–59 (2016)

48. S. Mallakpour, A. Abdolmaleki, H. Tabebordbar, Production of PVC/α-MnO_2-KH550 nanocomposite films: morphology, thermal, mechanical and Pb(II) adsorption properties. Eur. Polym. J. **78**, 141–152 (2016)

49. S. Mallakpour, F. Motirasoul, Preparation of PVA/α-MnO_2-KH550 nanocomposite films and study of their morphology, thermal, mechanical and Pb(II) adsorption properties. Prog. Org. Coat. **103**, 135–142 (2017)

50. S. Mallakpour, F. Motirasoul, Covalent surface modification of α-MnO_2 nanorods with L-valine amino acid by solvothermal strategy, preparation of PVA/α-MnO_2-L-valine nanocomposite films and study of their morphology, thermal, mechanical, Pb (ii) and Cd (ii) adsorption properties. RSC Adv **6**, 62602–62611 (2016)

51. S. Mallakpour, M. Madani, Use of valine amino acid functionalized α-MnO_2/chitosan bionanocomposites as potential sorbents for the removal of lead (II) ions from aqueous solution. Ind. Eng. Chem. Res. **55**, 8349–8356 (2016)

52. A. Abdolmaleki, S. Mallakpour, H. Tabebordbar, Improvement of PVC/α-MnO_2–LVA nanocomposites properties: a promising adsorbent for Pb(II) uptake. Int. J. Polym. Anal. Charact. **32**(2), 1–14 (2017)

53. S. Mallakpour, V. Behranvand, Sono-assisted preparation of bio-nanocomposite for removal of Pb^{2+} ions: study of morphology, thermal and wettability properties. Ultrason. Sonochem. **39**, 872–882 (2017)

54. S. Mallakpour, A. Abdolmaleki, F. Tabesh, Ultrasonic-assisted manufacturing of new hydrogel nanocomposite biosorbent containing calcium carbonate nanoparticles and tragacanth gum for removal of heavy metal. Ultrason. Sonochem. **41**, 572–581 (2018)

55. R.P. Mason, J.R. Reinfelder, F.M. Morel, Uptake, toxicity, and trophic transfer of mercury in a coastal diatom. Environ. Sci. Technol. **30**, 1835–1845 (1996)

56. J. Wang, B. Deng, H. Chen, X. Wang, J. Zheng, Removal of aqueous Hg(II) by polyaniline: sorption characteristics and mechanisms. Environ. Sci. Technol. **43**, 5223–5228 (2009)

57. M. Teng, H. Wang, F. Li, B. Zhang, Thioether-functionalized mesoporous fiber membranes: sol–gel combined electrospun fabrication and their applications for Hg^{2+} removal. J. Colloid Interface Sci. **355**, 23–28 (2011)

58. S. Li, X. Yue, Y. Jing, S. Bai, Z. Dai, Fabrication of zonal thiol-functionalized silica nanofibers for removal of heavy metal ions from wastewater. Colloids Surf. A Physicochem. Eng. Asp. **380**, 229–233 (2011)

59. P.T. Tanev, T.J. Pinnavaia, A neutral templating route to mesoporous molecular sieves. Science **267**, 865–867 (1995)

60. H. Javadian, M. Ghaemy, M. Taghavi, Adsorption kinetics, isotherm, and thermodynamics of Hg^{2+} to polyaniline/hexagonal mesoporous silica nanocomposite in water/wastewater. J. Mater. Sci. **49**, 232–242 (2014)

61. X. Wang, L. Yang, J. Zhang, C. Wang, Q. Li, Preparation and characterization of chitosan–poly (vinyl alcohol)/bentonite nanocomposites for adsorption of Hg(II) ions. Chem. Eng. J. **251**, 404–412 (2014)

62. P. Monvisade, P. Siriphannon, Chitosan intercalated montmorillonite: preparation, characterization and cationic dye adsorption. Appl. Clay. Sc. **42**, 427–431 (2009)

63. V.P. Cyras, L.B. Manfredi, M.-T. Ton-That, A. Vázquez, Physical and mechanical properties of thermoplastic starch/montmorillonite nanocomposite films. Carbohydr. Polym. **73**, 55–63 (2008)

64. P.C. Gomes, M.P. Fontes, A.G. da Silva, E. de S Mendonça, A.R. Netto, Selectivity sequence and competitive adsorption of heavy metals by Brazilian soils. Soil Sci. Soc. Am. J. **65**(4), 1115–1121 (2001)

65. P. Anderson, T.H. Christensen, Distribution coefficients of Cd Co, Ni, and Zn in soils. Eur. J. Soil Sci. **39**, 15–22 (1988)

66. Y. Lin, G.E. Fryxell, H. Wu, M. Engelhard, Selective sorption of cesium using self-assembled monolayers on mesoporous supports. Environ. Sci. Technol. **35**, 3962–3966 (2001)

67. A.H. Dam, D. Kim, Metal ion-imprinted polymer microspheres derived from copper methacrylate for selective separation of heavy metal ions. J. Appl. Polym. Sci. **108**, 14–24 (2008)

68. S.K. Singh, K.Y. Rhee, S.-Y. Lee, S.-J. Park, Facile fabrication of Poly (vinyl alcohol)/Silica composites for removal of Hg(II) from water. Macromol. Res. **23**, 21–29 (2015)

69. S. Lopez-Orozco, A. Inayat, A. Schwab, T. Selvam, W. Schwieger, Zeolitic materials with hierarchical porous structures. Adv. Mater. **23**, 2602–2615 (2011)

70. H. Javadian, M. Taghavi, Application of novel Polypyrrole/thiol-functionalized zeolite Beta/MCM-41 type mesoporous silica nanocomposite for adsorption of Hg^{2+} from aqueous solution and industrial wastewater: kinetic, isotherm and thermodynamic studies. Appl. Surf. Sci. **289**, 487–494 (2014)

71. M.P. Waalkes, Cadmium carcinogenesis in review. J. Inorg. Biochem. **79**, 241–244 (2000)

72. B.L. Vallee, D.D. Ulmer, Biochemical effects of mercury, cadmium, and lead. Annu. Rev. Biochem. **41**, 91–128 (1972)

73. V. Singh, A. Tiwari, D.N. Tripathi, R. Sanghi, Microwave assisted synthesis of guar-g-polyacrylamide. Carbohydr. Polym. **58**, 1–6 (2004)

74. V. Singh, S. Pandey, S. Singh, R. Sanghi, Removal of cadmium from aqueous solutions by adsorption using poly (acrylamide) modified guar gum–silica nanocomposites. Sep. Purif. Technol. **67**, 251–261 (2009)

75. L.Z. Zhang, P. Cheng, G.-Q. Tang, D.-Z. Liao, Electronic properties of an organic molecule within MCM-41 host: a spectroscopic and theoretical study toward elucidating the variation in band gaps of the guest species. J. Lumin. **104**, 123–129 (2003)

76. H. Yang, Y. Deng, C. Du, Synthesis and optical properties of mesoporous MCM-41 containing doped TiO_2 nanoparticles. Colloids Surf. A Physicochem. Eng. Asp. **339**, 111–117 (2009)

77. A.N. Chermahini, M.K. Omran, H.A. Dabbagh, G. Mohammadnezhad, A. Teimouri, Application of a functionalized mesoporous silica catalyst to the synthesis of tetrazoles. New J. Chem. **39**, 4814–4820 (2015)

78. M. Kruk, M. Jaroniec, A. Sayari, Application of large pore MCM-41 molecular sieves to improve pore size analysis using nitrogen adsorption measurements. Langmuir **13**, 6267–6273 (1997)

79. G. Mohammadnezhad, M. Dinari, R. Soltani, Z. Bozorgmehr, Thermal and mechanical properties of novel nanocomposites from modified ordered mesoporous carbon FDU-15 and poly (methyl methacrylate). Appl. Surf. Sci. **346**, 182–188 (2015)

80. M. Vallet-Regi, A. Ramila, R. Del Real, J. Pérez-Pariente, A new property of MCM-41: drug delivery system. Chem. Mater. **13**, 308–311 (2001)

81. G. Mohammadnezhad, S. Abad, R. Soltani, M. Dinari, Study on thermal, mechanical and adsorption properties of amine-functionalized MCM-41/PMMA and MCM-41/PS nanocomposites prepared by ultrasonic irradiation. Ultrason. Sonochem. **39**, 765–773 (2017)

82. M. Dinari, G. Mohammadnezhad, A. Nabiyan, Preparation and characterization of nanocomposite materials based on

83. polyamide-6 and modified ordered mesoporous silica KIT-6. J. Appl. Polym. Sci. **133**, 43098 (2016)

83. M. Dinari, G. Mohammadnezhad, A. Nabiyan, Organo-modified mesoporous carbon FDU-15 as new nanofiller for the preparation of nanocomposite materials based on nylon-6. Colloid Polym. Sci. **293**, 1569–1575 (2015)

84. G. Mohammadnezhad, R. Soltani, S. Abad, M. Dinari, A novel porous nanocomposite of aminated silica MCM-41 and nylon-6: isotherm, kinetic, and thermodynamic studies on adsorption of Cu (II) and Cd (II). J. Appl. Polym. Sci. **134**, 45383 (2017)

85. R. Soltani, M. Dinari, G. Mohammadnezhad, Ultrasonic-assisted synthesis of novel nanocomposite of poly (vinyl alcohol) and amino-modified MCM-41: a green adsorbent for Cd (II) removal. Ultrason. Sonochem. **40**, 533–542 (2018)

86. M. Dinari, G. Mohammadnezhad, R. Soltani, Fabrication of poly (methyl methacrylate)/silica KIT-6 nanocomposites via in situ polymerization approach and their application for removal of Cu^{2+} from aqueous solution. RSC Adv. **6**, 11419–11429 (2016)

87. A. Heidari, H. Younesi, Z. Mehraban, Removal of Ni (II), Cd (II), and Pb(II) from a ternary aqueous solution by amino functionalized mesoporous and nano mesoporous silica. Chem. Eng. J. **153**, 70–79 (2009)

88. M. Najafi, Y. Yousefi, A. Rafati, Synthesis, characterization and adsorption studies of several heavy metal ions on amino-functionalized silica nano hollow sphere and silica gel. Sep. Purif. Technol. **85**, 193–205 (2012)

89. G. Venkatesh, A.K. Singh, B. Venkataramani, Silica gel loaded with o-dihydroxybenzene: design, metal sorption equilibrium studies and application to metal enrichment prior to determination by flame atomic absorption spectrometry. Microchim. Acta **144**, 233–241 (2004)

90. A. Goswami, A.K. Singh, 1, 8-Dihydroxyanthraquinone anchored on silica gel: synthesis and application as solid phase extractant for lead (II), zinc (II) and cadmium (II) prior to their determination by flame atomic absorption spectrometry. Talanta **58**, 669–678 (2002)

91. D.Q. Melo, V.O. Neto, J.T. Oliveira, A.L. Barros, E.C. Gomes, G.S. Raulino, E. Longuinotti, R.F. Nascimento, Adsorption equilibria of Cu^{2+}, Zn^{2+}, and Cd^{2+} on EDTA-functionalized silica spheres. J. Chem. Eng. Data **58**, 798–806 (2013)

92. M. Machida, B. Fotoohi, Y. Amamo, T. Ohba, H. Kanoh, L. Mercier, Cadmium (II) adsorption using functional mesoporous silica and activated carbon. J. Hazard. Mater. **221**, 220–227 (2012)

93. A. Abdolmaleki, S. Mallkpour, H. Tabebordbar, Study on morphology, thermal, mechanical and Cd (II) adsorption properties of PVC/α-MnO_2-stearic acid nanocomposites: production and application. J. Polym. Res. **23**, 260 (2016)

94. S. Mallakpour, F. Motirasoul, Use of PVA/α-MnO_2-stearic acid nanocomposite films prepared by sonochemical method as a potential sorbent for adsorption of Cd (II) ion from aqueous solution. Ultrason. Sonochem. **37**, 623–633 (2017)

95. S. Mallakpour, F. Motirasoul, Ultrasonication synthesis of PVA/PVP/α-MnO_2-stearic acid blend nanocomposites for adsorbing CdII ion. Ultrason. Sonochem. **40**, 410–418 (2018)

96. S. Mallakpour, F. Motirasoul, Bio-functionalizing of α-$MnO2$ nanorods with natural L-amino acids: a favorable adsorbent for the removal of Cd (II) ions. Mater. Chem. Phys. **191**, 188–196 (2017)

97. X. Yuan, Q. Jing, J. Chen, L. Li, Photocatalytic Cr(VI) reduction by mixed metal oxide derived from ZnAl layered double hydroxide. Appl. Clay Sc. **143**, 168–174 (2017)

98. S. Mallakpour, M. Hatami, Biosafe organic diacid intercalated LDH/PVC nanocomposites versus pure LDH and organic diacid intercalated LDH: synthesis, characterization and removal

behaviour of Cd^{2+} from aqueous test solution. Appl. Clay Sc. **149**, 28–40 (2017)

99. S. Mallakpour, E. Khadem, Poly (vinyl alcohol)/CaCO3-diacid nanocomposite: investigation of physical and wetting properties and application in heavy metal adsorption. J. Appl. Polym. Sci. **134**, 45414 (2017)

100. S. Mallakpour, V. Behranvand, Recycled PET/MWCNT-ZnO quantum dot nanocomposites: adsorption of Cd (II) ion, morphology, thermal and electrical conductivity properties. Chem. Eng. J. **313**, 873–881 (2017)

101. S. Mallakpour, A.N. Ezhieh, Effect of Starch-MWCNT@ Valine Nanocomposite on the Optical, Morphological, Thermal, and Adsorption Properties of Chitosan. J. Polym. Environ. **25**, 875–883 (2017)

102. S. Mallakpour, V. Behranvand, Water Sanitization by the Elimination of Cd^{2+} Using Recycled PET/MWNT/LDH Composite: morphology, Thermal, Kinetic, and Isotherm Studies. ACS Sustain. Chem. Eng. **5**, 5746–5757 (2017)

103. S. Mallakpour, V. Behranvand, Application of recycled PET/carboxylated multi-walled carbon nanotube composites for Cd^{2+} adsorption from aqueous solution: a study of morphology, thermal stability, and electrical conductivity. Colloid Polym. Sci. **295**, 453–462 (2017)

104. Chromium in Drinking-water Background document for development of WHO Guidelines for Drinking-water Quality, https://www.who.int/water_sanitation_health/dwq/chemicals/chromium.pdf

105. G.R. Wilson, A. Sharma, D. Sachdev, A. Dubey, Ferulic acid functionalized mesoporous silica polymer nanocomposites (SBA/FA) for the adsorption of Cr(VI). J. Porous Mater. **23**, 195–200 (2016)

106. F.-M. Pellera, A. Giannis, D. Kalderis, K. Anastasiadou, R. Stegmann, J.-Y. Wang, E. Gidarakos, Adsorption of Cu (II) ions from aqueous solutions on biochars prepared from agricultural by-products. J. Environ. Manage. **96**, 35–42 (2012)

107. A.E. Chávez-Guajardo, J.C. Medina-Llamas, L. Maqueira, C.A. Andrade, K.G. Alves, C.P. de Melo, Efficient removal of Cr(VI) and Cu (II) ions from aqueous media by use of polypyrrole/maghemite and polyaniline/maghemite magnetic nanocomposites. Chem. Eng. J. **281**, 826–836 (2015)

108. H. Wang, X. Yuan, Y. Wu, X. Chen, L. Leng, H. Wang, H. Li, G. Zeng, Facile synthesis of polypyrrole decorated reduced graphene oxide–Fe3O4 magnetic composites and its application for the Cr(VI) removal. Chem. Eng. J. **262**, 597–606 (2015)

109. M. Dinari, R. Soltani, G. Mohammadnezhad, Kinetics and Thermodynamic Study on Novel Modified-Mesoporous Silica MCM-41/Polymer Matrix Nanocomposites: effective Adsorbents for Trace CrVI Removal. J. Chem. Eng. Data **62**, 2316–2329 (2017)

110. V.K. Gupta, A. Rastogi, A. Nayak, Biosorption of nickel onto treated alga (Oedogonium hatei): application of isotherm and kinetic models. J. Colloid Interface Sci. **342**, 533–539 (2010)

111. H. Javadian, P. Vahedian, M. Toosi, Adsorption characteristics of Ni (II) from aqueous solution and industrial wastewater onto polyaniline/HMS nanocomposite powder. Appl. Surf. Sci. **284**, 13–22 (2013)

112. E. Borai, M. Breky, M. Sayed, M. Abo-Aly, Synthesis, characterization and application of titanium oxide nanocomposites for removal of radioactive cesium, cobalt and europium ions. J. Colloid Interface Sci. **450**, 17–25 (2015)

113. Basic Information about Copper in Drinking Water, Environmental Protection Agency (2013)

114. G. Mohammadnezhad, M. Dinari, A. Nabiyan, High Surface Area Nano-Boehmite as Effective Nano-Filler for Preparation of Boehmite-Polyamide-6 Nanocomposites. Adv. Polym. Tech. **37**, 1221–1228 (2016)

115. G. Mohammadnezhad, M. Dinari, R. Soltani, The preparation of modified boehmite/PMMA nanocomposites by in situ polymerization and the assessment of their capability for Cu^{2+} ion removal. New J. Chem. **40**, 3612–3621 (2016)

116. G. Mohammadnezhad, P. Moshiri, M. Dinari, F. Steiniger, In situ synthesis of nanocomposite materials based on modified mesoporous silica MCM-41 and methyl methacrylate for copper (II) adsorption from aqueous solution. JICS **16**, 1491–1500 (2019)

117. S. Mallakpour, E. Khadem, Facile and cost-effective preparation of PVA/modified calcium carbonate nanocomposites via ultrasonic irradiation: application in adsorption of heavy metal and oxygen permeation property. Ultrason. Sonochem. **39**, 430–438 (2017)

118. S. Mallakpour, E. Khadem, Chitosan reinforced with modified $CaCO_3$ nanoparticles to enhance thermal, hydrophobicity properties and removal of cu (II) and cd (II) ions. J. Polym. Res. **24**, 86 (2017)

119. S. Mallakpour, A. Nezamzadeh Ezhieh, Preparation and characterization of starch nanocomposite embedded with functionalized MWCNT: Investigation of optical, morphological, thermal, and copper ions adsorption properties. Adv. Polym. Tech. **37**, 2195–2203 (2017)